Studies on the interaction between substances derived from pathogens and an antimicrobial peptide tachyplesin I

（病原菌由来物質と抗菌ペプチドタキプレシン I の相互作用に関する研究）

Graduate School of Life Science

Hokkaido University

2015

Takahiro Kushibiki

Contents

Abbreviations

AMPs	antimicrobial peptides
CD	circular dichroism
DMSO	dimethyl sulfoxide
DPC	dodecylphosphocholine
HPLC	high performance liquid chromatography
LPS	lipopolysaccharide
MALDI	matrix assisted laser desorption ionization
NMR	nuclear magnetic resonance
SDS	sodium dodecyl sulfate
TOCSY	total correlation spectroscopy
TOF MS	time of flight mass spectroscopy
TP I	tachyplesin I
Tr-NOESY	transfer nuclear Overhauser effect spectroscopy
RMSD	root-mean-square deviation

Abstract

A wide variety of organisms have antimicrobial peptides (AMPs) as part of their innate immune system. AMPs exhibit broad spectrum antimicrobial activity and have a low propensity for eliciting the development of resistance in bacteria; they have thus become promising as potential new antibiotics. On the basis of their secondary structures, AMPs can be broadly classified into three groups, α-helical peptides, β-sheet peptides, and flexible peptides. α-helical peptides are the most extensively characterized, whereas there is insufficient knowledge about β-sheet peptides. In particular, the interaction between substances derived from pathogens and AMPs and the structural information at the complex-formation are poorly understood.

In part I of this thesis, I investigated the structure of tachyplesin I (TP I) in the presence of lipopolysaccharide (LPS) and proposed a model structure of the complex between them. LPS is a major constituent of the outer membrane of Gram-negative bacteria and is the very first site of interactions with AMPs. In order to gain better insight into the interaction between LPS and AMPs, I determined the structure of TP I, an antimicrobial peptide derived from horseshoe crab, in its bound state with LPS and proposed the complex structure of TP I and LPS using a docking program. CD and NMR measurements revealed that binding to LPS slightly extends the two β-strands of TP I and stabilizes the whole structure of TP I. The fluorescence wavelength of an intrinsic tryptophan of TP I and fluorescence quenching in the presence or absence of LPS indicated that a tryptophan residue is incorporated into the hydrophobic environment of LPS. Finally, I succeeded in proposing a structural model for the complex of TP I and LPS by using a docking program. The calculated model structure suggested that the cationic residues of TP I interact with phosphate groups and saccharides of LPS, whereas hydrophobic residues interact with the

acyl chains of LPS.

In regard to α-helical peptides, there are a few reports on the complex structure of AMPs and LPS. However, no complex structure between LPS and β-sheet AMPs has been reported. It is noteworthy that this is the first structure of an AMP belonging to the β-sheet peptide in the LPS micelle.

In part II of this thesis, I investigated the structural factors or key residues that are important for TP I to bind to chitin. Chitin, a linear β-1,4-linked polymer of N-acetylglucosamine, is an essential component of fungal cell walls. Some AMPs are thought to exert their antifungal activity by binding to chitin, but the details of the interaction between them are less well studied. To gain better understanding of the chitin-binding ability of AMPs, I determined the chitin-binding site of TP I, an antimicrobial peptide isolated from horseshoe crab.

One-dimensional ^{1}H NMR study indicated that the four residues, F4, R9, Y13, and R17, of TP I may have the ability to interact with hexa-N-acetyl-chitiohexaose, the largest soluble derivative of chitin. I investigated the importance of these residues for chitin-binding by using TP I mutants. Based on the results of the chitin-binding assay of TP I and its mutants, it was confirmed that TP I can bind strongly to chitin. Meanwhile, the replacement of F4 and Y13 in particular attenuated the chitin-binding ability, and the mutant in which all four residues were replaced with Ala showed a marked reduction in chitin-binding ability. These results indicated that aromatic F4 and Y13 play the main role in binding of TP I to chitin, while cationic R9 and R17 are only secondarily involved in the binding.

To my knowledge, TP I is the shortest antimicrobial peptide that exhibits chitin-binding activity. My findings should help to clarify the mechanism of chitin-recognition of AMPs as well as the relationship between antifungal activity and chitin-binding activity.

General Introduction

Antimicrobial peptides (AMPs) have microbicidal properties and are a critical component of innate immunity [1-3]. To date, a large number of AMPs have been found in most living organisms, and over 2000 AMPs have currently been identified (see http://aps.unmc.edu/AP/main.php). In general, AMPs have the following common features. (1) AMPs are relatively short peptides with 12-100 amino acids. (2) AMPs are positively charged, with net charges of +2- +9 due to the presence of basic amino acids (Lys and Arg). (3) AMPs also have hydrophobic residues and often adopt an amphipathic structure. (4) AMPs are effective against a broad spectrum of pathogens, including Gram-negative and -positive bacteria, mycobacteria, fungi, parasites, and certain enveloped viruses [4-6].

Although several AMPs target intracellular molecules such as DNA, RNA, and heat shock protein [7-9], most AMPs exert their antimicrobial activity by interacting with and disrupting the bacterial cell membrane [10-16].

Recent studies have proposed several mechanisms of membrane-disruption, such as the “barrel-stave,” “toroidal pore” and “carpet” models [17, 18]. In the barrel-stave model, AMPs insert themselves into the bacterial membrane in a perpendicular orientation and form transmembrane pores by performing this insertion collectively in bundles [19, 20]. In the toroidal pore model, AMPs insert themselves perpendicular to the bacterial membrane and form pores involving phospholipid head groups [21, 22]. In the carpet model, AMPs aggregate parallel to the lipid bilayer. Then, the AMPs act in a detergent-like manner to break off the membrane lipids into micelles [23, 24]. There are a variety of other models as well. In order to clarify the antimicrobial mechanism in detail, structural studies of AMPs will be needed.

On the basis of their secondary structures, AMPs are categorized into three broad

types—namely, α-helical peptides, β-sheet peptides containing Cys residues, and flexible peptides rich in certain amino acids such as Trp [6].

Alpha-helical-type peptides are the most widely distributed AMPs. According to the AMP database (http://aps.unmc.edu/AP/main.php), there are over 300 α-helical AMPs. This type includes tempolins [25-28], aureins [29, 30], magainin [31, 32], cecropins [33-36], fowlicidin [37, 38], melittin [39-41], lasioglossin [42], lasiocepsin [43, 44], dermaseptins [45-49] and so on (Fig. 1). These peptides are often unstructured in water, but adopt an α-helical structure in membrane mimetic environments, such as in 1, 1, 1, 3, 3, 3-hexafluoro-2-propanol, sodium dodecyl sulfate (SDS) micelles and dodecylphosphocholine (DPC) micelles. The polar side chains align along one side and the hydrophobic residues along the opposite side of the helical coat. This amphipathic helical structure is thought to be important for interaction with the amphiphilic biological membrane [50].

AMPs categorized as β-sheet peptides are a secondary major group after the α-helical type. About 100 β-sheet type AMPs have been identified (http://aps.unmc.edu/AP/main.php). Tachyplesins [51-55], polyphemusin [56-58], gomesin [59, 60], thanatin [61, 62], defensin [63-65], protegrin [66, 67], and arenicin [68, 69] are perhaps the best-known of the β-type AMPs (Fig. 2). They are rich in cysteine residues which form disulfide bridges. Depending on their cysteine residues and disulfide bonds, they adopt a β-sheet structure with triple strands or a β-hairpin structure stabilized by disulfide bonds both in water and membrane mimetic environments [70].

Flexible peptides comprise a minor group of AMPs. There are only 9 AMPs categorized in this type in the AMPs database (http://aps.unmc.edu/AP/main.php). Indolicidin [71, 72], tritrpticin [73, 74], pyrrhocoricin [75, 76], drosocin [77, 78], nisin A [79], and diptericin [80, 81] are known as flexible peptides (Fig. 3). They often have an excess number of certain amino acids. For example, indolicidin and tritrpticin are rich in

Trp residues and pyrrhocoricin and drosocin are Pro-rich peptides. These peptides have a largely extended conformation even in membrane mimetic environments such as SDS and DPC micelles.

The emergence of drug-resistant bacteria has caused a major dilemma for human health care, and thus the development of antimicrobial peptides as a possible novel therapeutic approach for the treatment of infections is being actively pursued. Antimicrobial-based therapies are attractive candidates as alternative antibiotics, since they offer several potential advantages over the currently used classes of drugs. First, AMPs are naturally occurring agents that can rapidly respond to pathogens. Secondly, because they exploit fundamental structural characteristics such as the bacterial cell membrane or they have multiple targets within cells, the emergence of resistance is thought to be considerably reduced compared with that for many current antibiotics, which have specific molecular targets [4].

As an example of research aiming for the medical application of AMPs, analyses of the interaction between AMPs and LPS have received much attention [82-85]. LPS is a main component of the outer membrane of Gram-negative bacteria and is known as an endotoxin causing septic shock in humans [86]. Sepsis is a serious cause of clinical mortality, but no effective medical therapy has been established. Thus AMPs that can bind to LPS and prevent sepsis are expected to be applied in medicine.

Fowlicidin-1 is an AMP of chicken found in 2006 and exhibits potent activity against Gram-positive and –negative bacteria and LPS-neutralizing activity [87]. From the results of CD measurements, it was clarified that fowlicidin-1 is unstructured in aqueous solution but adopts an α-helical conformation in the presence of TFE or SDS [37]. The same report showed that fowlicidin-1 has at least two LPS-binding regions. These two fragments showed LPS-neutralizing activity and antimicrobial activity. In 2008, the complex models of these two α-helical active fragments combined with LPS were determined using NMR

spectroscopy [88]. The authors expressed the opinion that this structural information might be helpful in understanding the mechanism of action of AMPs and for the development of structure-based novel antisepsis analogs.

Pardaxin is a pore-forming membrane-active peptide isolated from Red Sea Moses sole fish [89]. Pardaxin was found to have antimicrobial activity against both Gram-positive and –negative bacteria [90]. The solution structure and LPS-bound structure were determined by CD measurements and NMR measurements in 2010 [91]. In this paper, the authors showed that pardaxin is mostly unstructured in aqueous solution and adopts a helical hairpin structure in the presence of LPS. The authors remarked that the complex model would be useful in the development of new antimicrobials with enhanced binding affinity for LPS.

AMPs may also be potentially useful in conjunction with existing drugs as a "combination therapy" to create an additive or synergistic effect.

Tachyplesin III is an AMP isolated from the hemolymph of the Southeast Asian horseshoe crabs *Tachypleus gigas* and *Carcinoscorpius rotundicauda* [92]. Tachyplesin III shows broad-spectrum activity against Gram-positive and –negative bacteria. Cirioni et al. investigated the efficacy of tachyplesin III and clarithromycin, an antibiotic that is useful for the treatment of a number of bacterial infections, in rat models of Gram-negative bacterial infection [93]. Tachyplesin III exerted a strong antimicrobial and anti-inflammatory activity, while clarithromycin exerted low antimicrobial activity but showed anti-inflammatory activity. By use of tachyplesin III in combination with clarithromycin, the antimicrobial and anti-inflammatory activity were significantly enhanced. This result suggests that membrane-active AMPs increase the permeability of the outer membrane and promote the penetration of antibiotics into bacteria. In 2009, Simonetti et al. confirmed that tachyplesin III has potential activity against dermatophytes [94]. They observed that the activity of tachyplesin III against dermatophytes is synergistically enhanced by the combination with terbinafine, an antifungal agent.

Several antimicrobial peptides have been developed and entered into clinical trials to date. Omiganan pentahydrochloride (MBI-226) is a cationic AMP composed of 12 amino acid residues. This peptide was synthesized based on indolicidin and showed antimicrobial activity against Gram-positive and -negative bacteria and fungi [95, 96]. Omiganan is one of the most developed AMPs, targeting the prevention of local catheter-site infections and catheter-related bloodstream infections. The gel preparation of omiganan is currently in phase III clinical trials.

Polimyxin B is an antibiotic substance isolated from *Bacillus polymyxa*. Polymyxin B has a unique specificity that exhibits no antimicrobial activity against Gram-positive bacteria but is active against Gram-negative bacteria [97]. This molecule is a cationic decapeptide containing six diaminobutyric acids and an acyl chain. Residues 4-10 make a heptapeptide cycle. The structures of polymyxin B in water and in LPS micelles were determined using NMR spectroscopy in 1999 [98]. In addition, the complex model of polymyxin and LPS was determined using NMR and molecular dynamics calculations in 2009 [99]. Although polymyxin B has nephrotoxicity and neurotoxicity [100], it has been used in clinical practice due to its effectiveness against multidrug-resistant Gram-negative bacteria.

While AMPs are promising substances as next-generation antibiotics and a few AMPs such as polymyxins are in clinical use, there are considerable challenges in the clinical application of AMPs in general, i.e., the hemolytic activity, susceptibility to proteolytic degradation, and high costs associated with peptide synthesis.

In order to overcome these disadvantages and design drugs with better therapeutic characteristics based on AMPs, analyses of the structural elements responsible for the antimicrobial action are indispensable.

In this thesis, I investigated the binding site and the complex structure between tachyplesin I (TP I) and substances derived from pathogens to gain a better understanding of

the interaction between them. TP I is found in small granules of hemocytes of the horseshoe crab *Tachypleus tridentatus* [51, 53]. TP I is a 17-residue peptide containing six cationic residues and two disulfide bonds (C3-C16 and C7-C12), and its C-terminus is amidated [51]. In water, TP I forms an antiparallel β-sheet structure [52, 54]. In part I of this thesis, I investigated the structure of TP I in the presence of LPS and proposed the model structure of the complex between them. In part II of this thesis, I investigated the structural factors or key residues that are important for TP I to bind to chitin, an essential component of fungal cell walls.

References

[1] P. Nicolas, A. Mor, Peptides as weapons against microorganisms in the chemical defense system of vertebrates, Annu. Rev. Microbiol. 49 (1995) 277-304.

[2] J.A. Hoffmann, Innate immunity of insects, Curr. Opin. Immunol. 7 (1995) 4-10.

[3] J.A. Hoffmann, J.M. Rehchhart, C. Hetru, Innate immunity in higher insects, Curr. Opin. Immunol. 8 (1996) 8-13.

[4] H. Jenssen, P. Hamill, R.E. Hancock, Peptide antimicrobial agents, Clin. Microbiol. Rev. 19 (2006) 491-511.

[5] Y. Huang, J. Huang, Y. Chen, Alpha-helical cationic antimicrobial peptides: relationships of structure and function, Protein Cell 1 (2010) 143-152.

[6] D. Takahashi, S.K. Shukla, O. Prakash, G. Zhang, Structural determinants of host defense peptides for antimicrobial activity and target cell selectivity, Biochimie 92 (2010) 1236-1241.

[7] L. Otvos Jr., O. Insug, M.E. Rogers, P.J. Consolvo, B.A. Condie, S. Lovas, P. Bulet, M. Blaszczyk-Thurin, Interaction between heat shock proteins and antimicrobial peptides, 39 (2000) 14150-14159.

[8] K.A. Brogden, Antimicrobial peptides: pore formers or metabolic inhibitors in bacteria? Nat. Rev. Microbiol. 3 (2005) 238-250.

[9] A. Anbanandam, D.C. Albarado, D.C. Tirziu, M. Simons, S. Veeraraghavan, Molecular basis for proline- and arginine-rich peptide inhibition of proteasome, J. Mol. Biol. 384 (2008) 219-227.

[10] M.M. Mahoney, A.Y. Lee, D.J. Brezinski-Caliguri, K.M. Huttner, Molecular analysis of the sheep cathelin family reveals a novel antimicrobial peptide, FEBS Lett. 377 (1995) 519-522.

[11] G. Wang, Structures of human host defense cathelicidin LL-37 and its smallest

antimicrobial peptide KR-12 in lipid micelles, J. Biol. Chem. 283 (2008) 32637-32643.

[12] J. Andrä, M.U. Hammer, J. Grötzinger, I. Jakovkin, B. Lindner, E. Vollmer, H. Fedders, M. Leippe, T. Gutsmann, Significance of the cyclic structure and of arginine residues for the antibacterial activity of arenicin-1 and its interaction with phospholipid and lipopolysaccharide model membranes, Biol. Chem. 390 (2009) 337-349.

[13] T. Kouno, M. Mizuguchi, T. Aizawa, H. Shinoda, M. Demura, S. Kawabata, K. Kawano, A novel beta-defensin structure: big defensin changes its N-terminal structure to associate with the target membrane, Biochemistry 48 (2009) 7629-7635.

[14] K.Hall, T.H. Lee, M.I. Aguilar, The role of electrostatic interactions in the membrane binding of melittin, J. Mol. Recognit. 24 (2011) 108-118.

[15] L.T. Nguyen, E.F. Haney, H.J. Vogel, The expanding scope of antimicrobial peptide structures and their modes of action, Trends Biotechnol. 29 (2011) 464-472.

[16] C.H. Lin, J.T. Tzen, C.L. Shyu, M.J. Yang, W.C. Tu, Structural and biological characterization of mastoparans in the venom of *Vespa* species in Taiwan, Peptides 32 (2011) 2027-2036.

[17] Y. Shai, Mechanism of the binding, insertion and destabilization of phospholipid bilayer membranes by alpha-helical antimicrobial and cell non-selective membrane-lytic peptides, Biochim. Biophys. Acta 1462 (1999) 55-70.

[18] L. Yang, T.A. Harroun, T.M. Weiss, L. Ding, H.W. Huang, Barrel-stave model or toroidal model? A case study on melittin pores, Biophys. J. 81 (2001) 1475-1485.

[19] H.W. Huang, Y. Wu, Lipid-alamethicin interactions influence alamethicin orientation, Biophys. J. 60 (1991) 1079-1087.

[20] H. Duclohier, G. Molle, J.Y. Dugast, G. Spach, Prolines are not essential residues in the “barrel-stave” model for ion channels induced by alamethicin analogues, Biophys. J. 63 (1992) 868-873.

[21] S.J. Ludtke, K. He, W.T. Heller, T.A. Harroun, L. Yang, H.W. Huang, Membrane pores

induced by magainin, Biochemistry 35 (1996) 13723-13728.

[22] Y. Imura, M. Nishida, Y. Ogawa, Y. Takakura, K. Matsuzaki, Action mechanism of tachyplesin I and effects of PEGylation, Biochim. Biophys. Acta, 1768 (2007) 1160-1169.

[23] E. Gazit, A. Boman, H.G. Boman, Y. Shai, Interaction of the mammalian antibacterial peptide cecropin P1 with phospholipid vesicles, Biochemistry 34 (1995) 11479-11488.

[24] Y. Shai, Molecular recognition between membrane-spanning polypeptides, Trends Biochem. Sci. 20 (1995) 460-464.

[25] A.K. Mahalka, P.K. Kinnunen, Binding of amphipathic alpha-helical antimicrobial peptides to lipid membranes: lessons from temporins B and L, Biochinica. Biophys. Acta 1788 (2009) 1600-1609.

[26] A. Bhunia, R. Saravanan, H. Mohanram, M.L. Mangoni, S. Bhattacharjya, NMR structures and interactions of temporin-1Tl and temporin-1Tb with lipopolysaccharide micelles: Mechanistic insights into outer membrane permeabilization and synergistic activity, J.Biol. Chem. 286 (2011) 24394-24406.

[27] A. Li, Y. Zhang, C. Wang, G. Wu, Z. Wang, Purification, molecular cloning, and antimicrobial activity of peptides from the skin secretion of the black-spotted frog, *Rana nigromaculata*, World J. Microbiol. Biotechnol. 29 (2013) 1941-1949.

[28] R. Saravanan, M. Joshi, H. Mohanram, A. Bhunia, M.L. Mangoni, S. Bhattacharjya, NMR structure of temporin-1 ta in lipopolysaccharide micelles: Mechanistic insight into inactivation by outer membrane, PloS One 8 (2013) e72718.

[29] T. Rozek, K.L.Wegener, J.H. Bowie, I.N. Olver, J.A. Carver, J.C. Wallace, M.J. Tyler, The antibiotic and anticancer active aurein peptides from the Australian Bell Frogs *Litoria aurea* and *Litoria raniformis* the solution structure of aurein 1.2, Eur. J. Biochem. 267 (2000) 5330-5341.

[30] S.R. Dennison, L.H. Morton, F. Harris, D.A. Phoenix, The interaction of aurein 2.5

with fungal membranes, Eur. Biophys. J. 43 (2014) 255-264.

[31] M. Zasloff, Magainins, a class of antimicrobial peptides from *Xenopus* skin: Isolation, characterization of two active forms, and partial cDNA sequence of a precursor, Proc. Natl. Acad. Sci. U S A. 84 (1987) 5449-5453.

[32] D. Marion, M. Zasloff, A. Bax, A two-dimensional NMR study of the antimicrobial peptide magainin 2, FEBS Lett. 227 (1988) 21-26.

[33] H. Steiner, Secondary structure of the cecropins: antibacterial peptides from the moth *Hyalophora cecropia*, FEBS Lett. 137 (1982) 283-287.

[34] D. Sipos, M. Andersson, A. Ehrenberg, The structure of the mammalian antibacterial peptide cecropin P1 in solution, determined by proton-NMR, Eur. J. Biochem. 209 (1992) 163-169.

[35] E. Gazit, I.R. Miller, P.C. Biggin, M.S. Sansom, Y. Shai, Structure and orientation of the mammalian antibacterial peptide cecropin P1 within phospholipid membranes, J. Mol. Biol. 258 (1996) 860-870.

[36] M. Andersson, A. Boman, H.G. Boman, *Ascaris* nematodes from pig and human make three antibacterial peptides: Isolation of cecropin P1 and two ASABF peptides, Cell. Mol. Life Sci., 60 (2003) 599-606.

[37] Y. Xiao, H. Dai, Y.R. Bommineni, J.L. Soulages, Y.X. Gong, O. Prakash, G. Zhang, Structure-activity relationships of fowlicidin-1, a cathelicidin antimicrobial peptide in chicken, FEBS J. 273 (2006) 2581-2593.

[38] Y.R. Bommineni, H. Dai, Y.X. Gong, J.L. Soulages, S.C. Fernando, U. Desilva, O. Prakash, G. Zhang, Fowlicidin-3 is an alpha-helical cationic host defense peptide with potent antibacterial and lipopolysaccharide-neutralizing activities, FEBS. J. 274 (2007) 418-428.

[39] T.C. Terwilliger, D. Eisenberg, The structure of melittin. I. Structure determination and partial refinement, J. Biol. Chem. 257 (1982) 6010-6015.

[40] T.C. Terwilliger, D. Eisenberg, The structure of melittin. II. Interpretation of the structure, J. Biol. Chem. 257 (1982) 6016-6022.

[41] H. Vogel, F. Jähnig, The structure of melittin in membranes, Biophys. J. 50 (1986) 573-582.

[42] V. Čeřovský, M. Buděšínský, O. Havorka, J. Cvačka, Z. Voburka, J. Slaninová, L. Borovičková, V. Fučík, L. Bednárová, I. Votruba, J. Straka, Lasioglossins: three novel antimicrobial peptides from the venom of the eusocial bee *Lasioglossum laticeps* (Hymenoptera: Halictidae), Chembiochem. 10 (2009) 2089-2099.

[43] L. Monincová, J. Slaninová, V. Fučík, O. Hovorka, Z. Voburka, L. Bednárová, P. Maloň, J. Štokrová, V. Čeřovský, Lasiocepsin, a novel cyclic antimicrobial peptide from the venom of eusocial bee *Lasioglossum laticeps* (Hymenoptera: Halictidae) Amino Acids 43 (2012) 751-761.

[44] L. Monincová, M. Buděšínský, S. Čujová, V. Čeřovský, V. Veverka, Structural basis for antimicrobial activity of lasiocepsin, Chembiochem. 24 (2014) 301-308.

[45] A. Mor, V.H. Nguyen, A. Delfour, D. Migliore-Samour, P. Nicolas, Isolation, amino acid sequence, and synthesis of dermaseptin, a novel antimicrobial peptide of amphibian skin, Biochemistry 30 (1991) 8824-8830.

[46] A. Mor, P. Nicolas, Isolation and structure of novel defensive peptides from frog skin, Eur. J. Biochem. 219 (1994) 145-154.

[47] A. Mor. M. Amiche, P. Nicolas, Structure, synthesis, and activity of dermaseptin b, a novel vertebrate defensive peptide from frog skin: relationship with adenoregulin, Biochemistry 33 (1994) 6642-6650.

[48] O. Lequin, F. Bruston, O. Convert, G. Chassaing, O. Nicolas, Helical structure of dermaseptin B2 in a membrane-mimetic environment, Biochemistry 42 (2003) 10311-10323.

[49] O. Lequin, A. Ladram, L. Chabbert, F. Bruston, O. Convert, D. Vanhoye, G. Chassaing,

P. Nicolas, M. Amiche, Dermaseptin S9, an alpha-helical antimicrobial peptide with a hydrophobic core and cationic termini, Biochemistry 45 (2006) 468-480.

[50] M. Dathe, T. Wieprecht, Structural features of helical antimicrobial peptides: their potential to modulate activity on model membranes and biological cells, Biochim. Biophys. Acta 1462 (1999) 71-87.

[51] T. Nakamura, H. Furunaka, T. Miyata, F. Tokunaga, T. Muta, S. Iwanaga, M. Niwa, T. Takao, Y. Shimonishi, Tachyplesin, a class of antimicrobial peptide from the hemocytes of the horseshoe crab (*Tachypleus tridentatus*). Isolation and chemical structure, J. Biol. Chem. 263 (1988) 16709-16713.

[52] K. Kawano, T. Yoneya, T. Miyata, K. Yoshikawa, F. Tokunaga, Y. Terada, S. Iwanaga, Antimicrobial peptide, tachyplesin I, isolated from hemocytes of the horseshoe crab (*Tachypleus tridentatus*). NMR determination of the beta-sheet structure, J. Biol. Chem. 265 (1990) 15365-15367.

[53] Y. Hirakura, S. Kobayashi, K. Matsuzaki, Specific interactions of the antimicrobial peptide cyclic beta-sheet tachyplesin I with lipopolysaccharides, Biochim. Biophys. Acta 1562 (2002) 32-36.

[54] A. Laederach, A.H. Andreotti, D.B. Fulton, Solution and micelle-bound structures of tachyplesin I and its active aromatic linear derivatives, Biochemistry 41 (2002) 12359-12368.

[55] T. Kushibiki, M. Kamiya, T. Aizawa, Y. Kumaki, T. Kikukawa, M. Mizuguchi, M. Demura, S. Kawabata, K. Kawano, Interaction between tachyplesin I, an antimicrobial peptide derived from horseshoe crab, and lipopolysaccharide, Biochim. Biophys. Acta 1844 (2014) 527-534.

[56] T. Miyata, F. Tokunaga, T. Yoneya, K. Yoshikawa, S. Iwanaga, M. Niwa, T. Takao, Y. Shimonishi, Antimicrobial peptides, isolated from horseshoe crab hemocytes, tachyplesin II, and polyphemusins I and II: chemical structures and biological activity,

J. Biochem. 106 (1989) 663-668.

[57] L. Zhang, M.G. Scott, H. Yan, L.D. Mayer, R.E. Hancock, Interaction of polyphemusin I and structural analogs with bacterial membranes, lipopolysaccharide, and lipid monolayers, Biochemistry 39 (2000) 14504-14514.

[58] J.P. Powers, A. Rozek, R.E. Hancock, Structure-activity relationships for the beta-hairpin cationic antimicrobial peptide polyphemusin I, Bichim. Biophys. Acta 1698 (2004) 239-250.

[59] P.I. Silva Jr., S. Daffre, P. Bulet, Isolation and characterization of gomesin, an 18-residue cysteine-rich defense peptide from the spider *Acanthoscurria gomesiana* hemocytes with sequence similarities to horseshoe crab antimicrobial peptides of the tachyplesin family, J. Biol. Chem. 275 (2000) 33464-33470.

[60] N. Mandard, P. Bulet, A. Caille, S. Daffre, F. Vovelle, The solution structure of gomesin, an antimicrobial cysteine-rich peptide from the spider, Eur. J. Biochem. 269 (2002) 1190-1198.

[61] P. Fehlbaum, P. Bulet, S. Chernysh, J.P. Briand, J.P. Roussel, L. Letellier, C. Hetru, J.A. Hoffmann, Structure-activity analysis of thanatin, a 21-residue inducible insect defense peptide with sequence homology to frog skin antimicrobial peptides, Proc. Natl. Acad. Sci. U S A. 93 (1996) 1221-1225.

[62] N. Mandard, P. Sodano, H. Labbe, J.M. Bonmatin, P. Bulet, C. Hetru, M. Ptak, F. Vovelle, Solution structure of thanatin, a potent bactericidal and fungicidal insect peptide, determined from proton two-dimensional nuclear magnetic resonance data, Eur. J. Biochem. 256 (1998) 404-410.

[63] K.J. Rosengren, N.L. Daly, L.M. Fornander, L.M. Jönsson, Y. Shirafuji, X. Qu, H.J. Vogel, A.J. Ouellette, D.J. Craik, Structural and functional characterization of the conserved salt bridge in mammalian paneth cell alpha-defensins: solution structures of mouse CRYPTDIN-4 and (E15D)-CRYPTDIN-4, J. Biol. Chem. 281 (2006)

28068-28078.

[64] A. Szyk, Z. Wu, K. Tucker, D. Yang, W. Lu, J. Lubkowski, Crystal structures of human alpha-defensins HNP4, HD5, and HD6, Protein Sci. 15 (2006) 2749-2760.

[65] A.J. Wommack, S.A. Robson, Y.A. Wanniarachchi, A. Wan, C.J. Turner, G. Wagner, E.M. Nolan, NMR solution structure and condition-dependent oligomerization of the antimicrobial peptide human defensin 5, Biochemistry 51 (2012) 9624-9637.

[66] V.N. Kokryakov, S.S. Harwig, E.A. Panyutich, A.A. Shevchenko, G.M. Aleshina, O.V. Shamova, H.A. Korneva, R.I. Lehrer, Protegrins: leukocyte antimicrobial peptides that combine features of corticostatic defensins and tachyplesins, FEBS Lett. 327 (1993) 231-236.

[67] R.L. Fahrner, T. Dieckmann, S.S. Harwig, R.I. Lehrer, D. Eisenberg, J. Feigon, Solution structure of protegrin-1, a broad-spectrum antimicrobial peptide from porcine leukocytes, Chem. Biol. 3 (1996) 543-550.

[68] T.V. Ovchinnikova, G.M. Aleshina, S.V. Balandin, A.D. Krasnosdembskaya, M.L. Markelov, E.I. Frolova, Y.F. Leonova, A.A. Tagaev, E.G. Krasnodembsky, V.N. Kokryakov, Purification and primary structure of two isoforms of arenicin, a novel antimicrobial peptide from marine polychaeta *Arenicola marina*, FEBS Lett. 577 (2004) 209-214.

[69] J.U. Lee, D.I. Kang, W.L. Zhu, S.Y. Shin, K.S. Hahm, Y. Kim, Solution structures and biological functions of the antimicrobial peptide, arenicin-1, and its linear derivative, Biopolymers 88 (2007) 208-216.

[70] P. Bulet, R. Stöcklin, L. Menin, Anti-microbial peptides: from invertebrates to vertebrates, Immunol. Rev. 198 (2004) 169-184.

[71] M.E. Selsted, M.J. Novotny, W.L. Morris, Y.Q. Tang, W. Smith, J.S. Cullor, Indolicidin, a novel bactericidal tridecapeptide amide from neutrophils, J. Biol. Chem. 267 (1992) 4292-4295.

[72] A. Rozek, C.L. Friendrich, R.E. Hancock, Structure of the bovine antimicrobial peptide indolicidin bound to dodecylphosphocholine and sodium dodecyl sulfate micelles, Biochemistry 39 (2000) 15765-15774.

[73] C. Lawyer, S. Pai, M. Watabe, P. Borgia, T. Mashimo, L. Eagleton, K. Watabe, Antimicrobial activity of a 13 amino acid tryptophan-rich peptide derived from a putative porcine precursor protein of a novel family of antibacterial peptides, FEBS Lett. 390 (1996) 95-98.

[74] D.J. Schibli, P.M. Hwang, H.J. Vogel, Structure of the antimicrobial peptide tritrpticin bound to micelles: a distinct membrane-bound peptide fold, Biochemistry 38 (1999) 16749-16755.

[75] S. Cociancich, A. Dupont, G. Hegy, R. Lanot, F. Holder, C. Hetru, J.A. Hoffmann, P. Bulet, Novel inducible antibacterial peptides from a hemipteran insect, the sap-sucking bug *Pyrrhocoris apterus*, Biochem. J. 300 (1994) 567-575.

[76] M. Zahn, N. Berthold, B. Kieslich, D. Knappe, R. Hoffmann, N. Sträter, Structural studies on the forward and reverse binding modes of peptides to the chaperone DnaK, J. Mol. Biol. 425 (2013) 2463-2479.

[77] P. Bulet, J.L. Dimarcq, C. Hetru, M. Lagueux, M. Charlet, G. Hegy, A. Van Dorsselaer, J.A. Hoffmann, A novel inducible antibacterial peptide of *Drosophila* carries an O-glycosylated substitution, J. Biol. Chem. 268 (1993) 14893-14897.

[78] A.M. McManus, L. Otvos Jr., R. Hoffmann, D.J. Craik, Conformational studies by NMR of the antimicrobial peptide, drosocin, and its non-glycosylated derivative: effects of glycosylation on solution conformation, Biochemistry, 38 (1999) 705-714.

[79] L.Y. Lian, W.C. Chan, S.D. Morley, G.C. Roberts, B.W. Bycroft, D. Jackson, Solution structures of nisin A and its two major degradation products determined by n.m.r., Biochem. J. 283 (1992) 413-420.

[80] K.A. Winans, D.S. King, V.R. Rao, C.R. Bertozzi, A chemically synthesized version of

the insect antibacterial glycopeptide, diptericin, disrupts bacterial membrane integrity, Biochemistry 38 (1999) 11700-11710.

[81] M. Cudic, P. Bulet, R. Hoffmann, D.J. Craik, L. Otvos Jr., Chemical synthesis, antibacterial activity and conformation of diptericin, an 82-mer peptide originally isolated from insects, Eur. J. Biochem. 266 (1999) 549-558.

[82] B.F. Tack, M.V. Sawai, W.R. Kearney, A.D. Robertson, M.A. Sherman, W. Wang, T. Hong, L.M. Boo, H. Wu, A.J. Waring, R.I. Lehrer, SMAP-29 has two LPS-binding sites and a central hinge, Eur. J. Biochem. 269 (2002) 1181-1189.

[83] P. Li, T. Wohland, B. Ho, J.L. Ding, Perturbation of lipopolysaccharide (LPS) micelles by sushi 3 (S3) antimicrobial peptide. The importance of an intermolecular disulfide bond in S3 dimer for binding, disruption, and neutralization of LPS, J. Biol. Chem. 279 (2004) 50150-50156.

[84] A. Bhunia, A. Ramamoorthy, S. Bhattacharjya, Helical hairpin structure of a potent antimicrobial peptide MSI-594 in lipopolysaccharide micelles by NMR spectroscopy, Chemistry 15 (2009) 2036-2040.

[85] R. Saravanan, H. Mohanram, M. Joshi, P.N. Domadia, J. Torres, C. Ruedl, S. Bhattacharjya, Structure, activity and interactions of the cysteine deleted analog of tachyplesin-1 with lipopolysaccharide micelle: Mechanistic insights into outer-membrane permeabilization and endotoxin neutralization, Biochim. Biophys. Acta 1818 (2012) 1613-1624.

[86] J. Cohen, The immunopathogenesis of sepsis, Nature 420 (2002) 885-891.

[87] Y. Xiao, Y. Cai, Y.R. Bommineni, S.C. Fernando, O. Prakash, S.E. Gilliland, G. Zhang, Identification and functional characterization of three chicken cathelicidins with potent antimicrobial activity, J. Biol. Chem. 281 (2006) 2858-2867.

[88] A. Bhunia, H. Mohanram, S. Bhattacharjya, Lipopolysaccharide bound structures of the active fragments of fowlicidin-1, a cathelicidin family of antimicrobial and

antiendotoxic peptide from chicken, determined by transferred nuclear Overhauser effect spectroscopy, Biopolymers 92 (2009) 9-22.

[89] Y. Shai, J. Fox, C. Caratsch, Y.L. Shih, C. Edwards, P. Lazarovici, Sequencing and synthesis of pardaxin, a polypeptide from the Red Sea Moses sole with ionophore activity, FEBS Lett. 242 (1988) 161-166.

[90] Z. Oren, Y. Shai, A class of highly potent antibacterial peptides derived from pardaxin, a pore-forming peptide isolated from Moses sole fish *Pardachirus marmoratus*, Eur. J. Biochem. 237 (1996) 303-310.

[91] A. Bhunia, P.N. Domadia, J. Torres, K.J. Hallock, A. Ramamoorthy, S. Bhattacharjya, NMR structure of pardaxin, a pore-forming antimicrobial peptide, in lipopolysaccharide micelles: mechanism of outer membrane permeabilization, J.Biol. Chem. 285 (2010) 3883-3895.

[92] T. Muta, T. Fujimoto, H. Nakajima, S. Iwanaga, Tachyplesins isolated from hemocytes of Southeast Asian horseshoe crabs (*Carcinoscorpius rotundicauda* and *Tachypleus gigas*): identification of a new tachyplesin, tachyplesin III, and a processing intermediate of its precursor, J. Biochem. 108 (1990) 261-266.

[93] O. Cirioni, R. Ghiselli, C. Silvestri, W. Kamysz, F. Orlando, A. Riva, E. Kamysz, S. Castelletti, M. Rocchi, V. Saba, G. Scalise, A. Giacometti, Efficacy of the combination of tachyplesin III and clarithromycin in rat models of *Escherichia coli* sepsis, Antimicrob. Agents Chemother. 52 (2008) 4351-4355.

[94] O. Simonetti, G. Ganzetti, D. Arzeni, A. Campanati, B. Marconi, C. Silvestri, O. Cirioni, E. Gabrielli, I. Lenci, W. Kamysz, E. Kamysz, A. Giacometti, G. Scalise, F. Barchiesi, A. Offidani, In vitro activity of tachyplesin III alone and in combination with terbinafine against clinical isolates of dermatophytes, Peptides 30 (2009) 1794-1797.

[95] H.S. Sader, K.A. Fedler, R.P. Rennie, S. Stevens, R.N. Jones, Omiganan pentahydrochloride (MBI 226), a topical 12-amino-acid cationic peptide: Spectrum of

antimicrobial activity and measurements of bactericidal activity, Antimicrob. Agents Chemother. 48 (2004) 3112-3118.

[96] T.R. Fritsche, P.R. Rhomberg, H.S. Sader, R.N. Jones, Antimicrobial activity of omiganan pentahydrochloride tested against contemporary bacterial pathogens commonly responsible for catheter-associated infections, J. Antimicrob. Chemother. 61 (2008) 1092-1098.

[97] P.G. Stansly, M.E. Schlosser, Studies on polymyxin: Isolation and identification of *Bacillus polymyxa* and differentiation of polymyxin from certain known antibiotics, J. Bacteriol. 54 (1947) 549-556.

[98] P. Pristovšek, J. Kidrič, Solution structure of polymyxins B and E and effect of binding to lipopolysaccharide: an NMR and molecular modeling study, J. Med. Chem. 42 (1999) 4604-4613.

[99] J. Mares, S. Kumaran, M. Gobbo, O. Zerbe, Interactions of lipopolysaccharide and polymyxin studied by NMR spectroscopy, J. Biol. Chem. 284 (2009) 11498-11506.

[100] M.E. Falagas, S.K. Kasiakou, Toxicity of polymyxins: a systematic review of the evidence from old and recent studies, Crit. Care 10 (2006) R27.

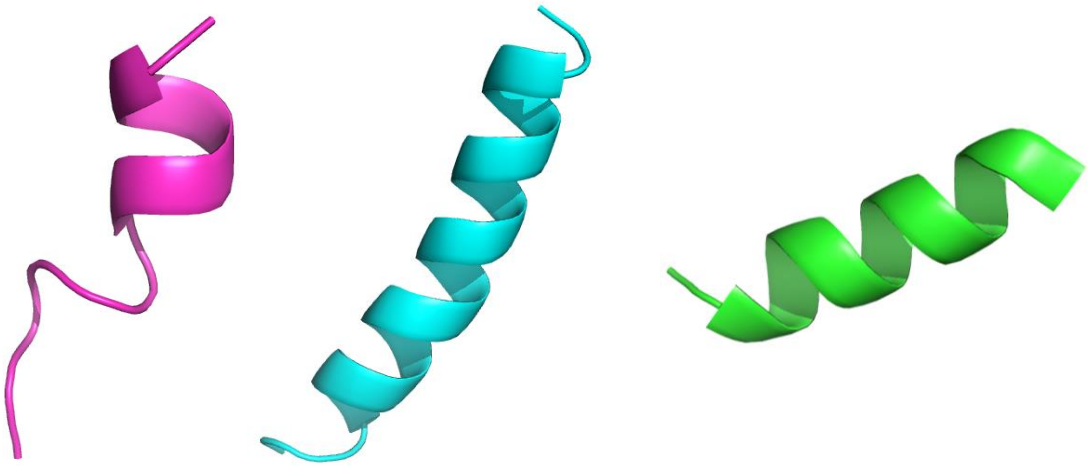

Figure 1. Structures of typical α-helical type AMPs: (a) tempolin-1Ta, (b) magainin2, (c) aurein1.2. All structures were determined by solution NMR spectroscopy.

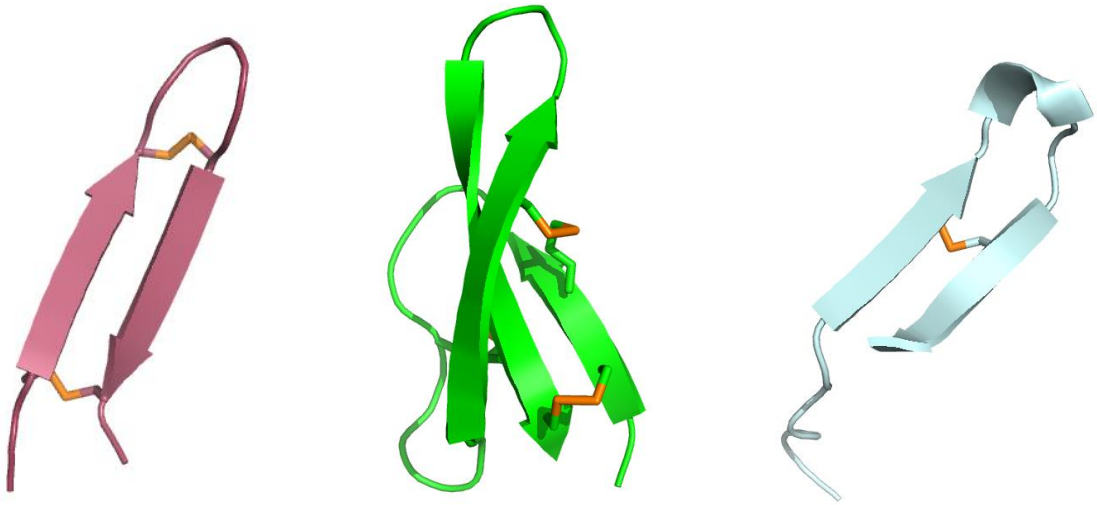

Figure 2. Structures of typical β-sheet type AMPs: (a) tachyplesin I, (b) thanatin, (c) human α-defensin 5. All structures were determined by solution NMR spectroscopy.

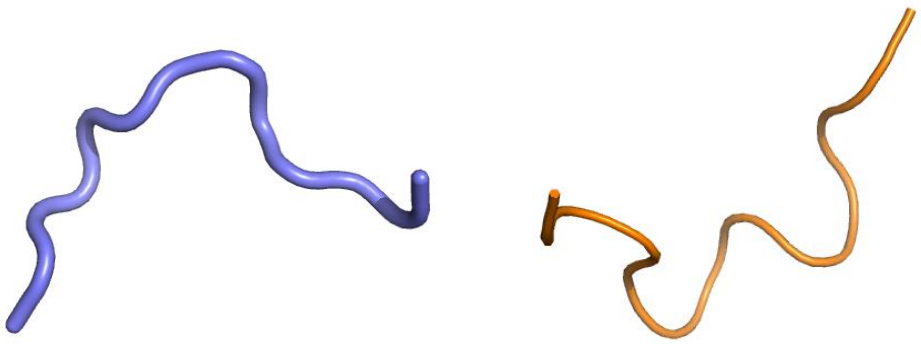

Figure 3. Structures of typical flexible-type AMPs: (a) indolicidin, (b) tritrpticin. All structures were determined by solution NMR spectroscopy.

Part I

Interaction between tachyplesin I, an antimicrobial peptide derived from horseshoe crab, and lipopolysaccharide

I-1 Abstract

Lipopolysaccharide (LPS) is a major constituent of the outer membrane of Gram-negative bacteria and is the very first site of interactions with antimicrobial peptides (AMPs). In order to gain better insight into the interaction between LPS and AMPs, I determined the structure of tachyplesin I (TP I), an antimicrobial peptide derived from horseshoe crab, in its bound state with LPS and proposed the complex structure of TP I and LPS using a docking program.

CD and NMR measurements revealed that binding to LPS slightly extends the two β-strands of TP I and stabilizes the whole structure of TP I. The fluorescence wavelength of an intrinsic tryptophan of TP I and fluorescence quenching in the presence or absence of LPS indicated that a tryptophan residue is incorporated into the hydrophobic environment of LPS. Finally, I succeeded in proposing a structural model for the complex of TP I and LPS by using a docking program. The calculated model structure suggested that the cationic residues of TP I interact with phosphate groups and saccharides of LPS, whereas hydrophobic residues interact with the acyl chains of LPS.

I-2 Introduction

Gram-negative bacteria have two kinds of membranes, an inner or cytoplasmic membrane composed of phospholipid bilayer and an outer membrane. The outer membrane of Gram-negative bacteria contains lipopolysaccharide (LPS) as a major component [1]. LPS occupies more than 90% of the outer membrane [2]. LPS consists of three distinct domains: the proximal, which is a hydrophobic lipid A region consisting of acyl chains connected to two phosphorylated glucosamine residues (GlcN); the distal, which is a highly variable polysaccharide moiety called the O-antigen; and a core oligosaccharide region that is covalently linked to the other two regions [1]. LPS is well known as an endotoxin, the inflammatory properties of which cause fatal septic shock in humans [3]. Sepsis has been a serious source of mortality in many clinical cases, but no effective medical therapy has been established. To overcome sepsis, antimicrobial peptides (AMPs) that interact with LPS have recently received increasing attention in the field of drug discovery [4,5].

AMPs are ubiquitously found in living organisms [6-9] and are an important component in innate immune response. Most AMPs exhibit a wide spectrum of antimicrobial activity against Gram-negative and Gram-positive bacteria, fungi, protozoa, and viruses [10]. In general, microbes are considered to have developed little or no resistance to AMPs unlike antibiotics, which have developed marked resistance [11]. Some AMPs that interact with LPS have been reported to neutralize endotoxin [12].

When AMPs exert their antimicrobial activity against Gram-negative bacteria or neutralize endotoxin, they should interact with the outer membrane components or LPS. Structural analyses of AMPs in complex with LPS are therefore important for understanding the mechanisms underlying the action of AMPs. However, although many structures of AMPs in water have been reported, there are just a few reports on the complex structure of AMPs-LPS or the structure of AMPs in the presence of LPS [5,13,14]. Details of the

interactions between AMPs and LPS and of the relationships between mechanisms of antimicrobial activity and their structures are still unclear.

Tachyplesin I (TP I) found in small granules of hemocytes of the horseshoe crab *Tachypleus tridentatus* is one of the AMPs that can bind to LPS [15,16]. TP I is a 17-residue peptide containing six cationic residues and two disulfide bonds (C3-C16 and C7-C12), and its C-terminus is amidated [15]. In water, TP I forms an antiparallel β-sheet structure [17,18]. The conformations of TP I in the presence of DPC micelles were also determined [18]. Furthermore, TP I mutants have been studied intensively. The structure of TPY4, a TP I mutant in which all the Cys residues are replaced with Tyr, has been revealed in water and in the presence of DPC micelles [18]. CDT is a mutant of TP I in which all Cys residues are deleted, and its LPS-bound structure has been determined [19]. However, the complex structure between wild-type TP I and LPS remains unclear. In order to obtain detailed structural information about the interaction between TP I and LPS, I investigated the structure of TP I in the presence of LPS by circular dichroism (CD) measurements, fluorescence experiments, nuclear magnetic resonance (NMR) measurements and docking calculation.

I-3 Materials and Methods

Peptide and reagents

TP I (KWCFRVCYRGICYRRCR-NH_2) was synthesized by Fmoc solid phase chemistry (Sigma Life Science). Based on the protocols of Powers et al. [20], I oxidized and purified TP I. In brief, TP I was dissolved in 20 mM Tris-HCl buffer (pH 8.0) and the solution was shaken for more than 24 hours at room temperature to promote disulfide bond formation by oxidation. The correctly folded TP I (C3-C16 and C7-C12) was then separated and purified by reverse-phase HPLC. Two disulfide bonds of the purified peptide were confirmed by MALDI-TOF mass spectroscopy through an observed 4 mass unit difference between the reduced and oxidized forms of TP I. Oxidized TP I solution was lyophilized and stored at -80 ºC. LPS of *Escherichia coli* O111:B4 was purchased from Sigma-Aldrich and was used without any further purification in all experiments.

Circular dichroism spectroscopy

CD spectra were recorded on a model J-725 spectropolarimeter (Jasco) using a quartz cell with a 1 mm path length. Spectra were measured at 25 ºC over the range from 190 to 250 nm at a scanning speed of 50 nm/min. TP I and LPS were dissolved in 10 mM sodium phosphate buffer (pH 7.4) and the concentrations were 30 μM and 72 μM, respectively. The contribution from the buffer was removed by subtracting the spectrum of a sample without TP I.

NMR spectroscopy

All NMR spectra were recorded either on a BRUKER DMX 500 MHz equipped with a cryo-probe or a JEOL ECA 600 MHz spectrometer. Data were processed using NMRPipe 4.1 and NMRDraw 2.3 [21] and analyzed using Sparky 3.113 software [22]. ^{1}H NMR

experiments were performed at 35 ºC with a TP I concentration of 750 μM in an aqueous solution containing 50 μM LPS and 10% D_2O, pH 3.8. The spectra of TP I in free solution were acquired at 1 mM peptide concentration. The mixing times of Two-dimensional TOCSY [23] and Tr-NOESY [24] spectra were 90 and 150 ms, respectively. The interaction of TP I with LPS was examined by measurements of 1D ^{31}P NMR at 35 ºC. 0.4 mM LPS in 10% D_2O at pH 3.8 was titrated using TP I at concentrations of 0.2, 0.4, and 0.6 mM. I confirmed that no oligomerization of the peptide is present under my experimental conditions (data not shown).

Calculation of the three-dimensional structure of TP I

In the presence and absence of LPS, a total of 216 and 110 distance restraints were acquired from the Tr-NOESY and NOESY spectra, respectively. The TP I structures with or without LPS micelles were calculated using XPLOR-NIH [25,26]. A total of 100 structures were calculated and the quality of the structures was checked with the program PROCHECK-NMR [27] for the 20 lowest-energy structures. Structures were visualized using PyMOL [28]. NMR resonance assignments for TP I in LPS and in water have been deposited in the BioMagResBank (BMRB) entry 11538 and 11539, respectively. The structural coordinates of TP I in LPS and in water have been deposited in the Protein Data Bank (PDB) ID 2MDB and 2RTV, respectively.

Tryptophan fluorescence studies

All fluorescence experiments were carried out using a 650-40 fluorescence spectrophotometer (Hitachi) and 1 cm path length cuvette.

TP I was dissolved in 10 mM sodium phosphate buffer (pH 7.4) and its concentration was 5 μM. The intrinsic tryptophan fluorescence emission spectra were obtained by titrating a stock solution of 1 mM LPS into a TP I solution. The exciting wavelength was set to 280

nm and emission was monitored from 300 to 500 nm at 25 ºC.

Fluorescence quenching experiments were performed by stepwise addition of acrylamide from a stock solution of 5 M into sample solution at 25 ºC. The sample solution contained 5 μM TP I and 12 μM LPS in sodium phosphate buffer at pH 7.4.

The results of the fluorescence quenching experiments were analyzed by fitting to the Stern-Volmer equation, $F_0 / F = 1 + K_{SV}[Q]$. F_0 and F are the fluorescence intensities at the appropriate emission wavelength in the absence and presence of acrylamide, respectively. K_{SV} is the Stern-Volmer quenching constant and [Q] is the molar concentration of acrylamide.

Docking of TP I with LPS

The structure of TP I calculated from the distance restraints of Tr-NOE was docked onto LPS by the program AutoDock 4.2 [29]. Docking calculations were carried out based on the protocols of Bhunia et al. [13]. The atomic coordinate of LPS (PDB ID 1QFG) used for docking calculations was obtained from the co-crystal structure of LPS and Fhu A [30]. The TP I was used as a ligand and backbone was kept rigid, whereas almost all side chains were defined as flexible. LPS was defined as a receptor and was kept rigid. Grid maps representing LPS were constructed using 70×80×80 points, with a grid spacing of 0.375 Å and grid center of the H2 atom of the GlcN II in lipid A. Docking calculation was carried out by using a Lamarchian genetic algorithm (LGA) with a translation step of 0.2 Å, a quaternion step of 5 deg, and a torsion step of 5 deg. The maximum number of energy evaluations increased to 15,000,000. 200 LGA docking runs were performed.

I-4 Results

Circular dichroism spectroscopy

I measured CD spectra of TP I in the presence or absence of LPS to estimate the secondary structures of TP I, and investigated whether TP I changes its conformation by binding to LPS. First, I measured CD spectra of TP I in the presence and absence of LPS at temperatures ranging from 25 °C to 40 °C and confirmed that there were no changes in the spectra (data not shown). The horseshoe crab is a heterothermic, saltwater animal, so I adopted the result at 25 °C. The spectrum of TP I in water displayed two positive bands at 198 and 232 nm and one negative band at 211 nm (Fig. 1). These bands are indicative of a β-sheet structure and a β-turn structure. This estimated structure of TP I in water is consistent with a previous report [16]. TP I in the presence of LPS also exhibited two positive bands at 204 and 232 nm and one negative band at 212 nm (Fig. 1). This spectrum indicated that TP I retains a β-sheet structure and a β-turn structure in its LPS-bound state. If none of the conformational changes are caused by binding to LPS, the spectrum of TP I fits with that of TP I in the presence of LPS. As is obvious from the spectra, the two spectra do not completely fit each other. This suggested that TP I changes its conformation by binding to LPS.

NMR studies of TP I in an aqueous solution

Although the solution structure of TP I was already clarified [17], to compare the structure of TP I in water with its LPS-bound state under the same condition, I measured 1D ^{1}H NMR, 2D TOCSY and NOESY of TP I in the absence of LPS and determined its solution structure (data not shown). ^{1}H resonance assignments of all the amino acids were obtained by the combined analyses of TOCSY and NOESY spectra. In aqueous solution, most of the chemical shift values of $^{1}H^{\alpha}$ were shifted down-field compared with the

random-coil shift values. This property indicated that TP I adopts a β-sheet structure. The NOESY spectrum showed the long range NOEs among residues C3/C16, F4/R15, F4/C16, R5/R14, R5/R15, V6/Y13, V6/R14, C7/C12 and C7/Y13. These NOEs suggested a two-stranded antiparallel structure of TP I. These results were well consistent with the previous reports.

Tr-NOESY of TP I in its LPS-bound state

To determine the structure of TP I in its LPS-bound state, I acquired 1D ^{1}H NMR, 2D TOCSY and Tr-NOESY spectra. The line-broadening of proton resonances was caused by the addition of 0.25 mg LPS into the solutions containing TP I (Fig. 2a). This line-broadening indicates a fast or intermediate exchange between free and LPS-bound states at the NMR time scale. I decided to measure Tr-NOESY spectra of TP I in the presence of LPS under the condition by which the line-broadening of TP I resonances was observed.

Tr-NOESY has the advantage that it can be used for the structural analysis of high-molecular-weight complexes that cannot be studied by other NMR measurements due to the broad line widths [24]. The critical micelle concentration (CMC) value of LPS has been estimated to be 1.3 ~ 1.6 μM [31], and LPS forms large micelles even at low concentrations, so the structural analysis of LPS-peptide complexes has not been easy. However, the observation of tr-NOEs from the LPS-bound peptides enabled us to determine the structure of the peptides in their LPS-bound state. By contrast to the NOESY spectrum of TP I without LPS, the number of NOE cross-peaks of TP I drastically increased in the presence of LPS (Fig. 2b). The numbers of NOEs of TP I in water and in the presence of LPS are summarized in Fig. 3. The increased peaks were mainly for sequential and inter-residue (>i+1) NOEs. Figure 3 shows that the NOEs of Cys3 and Arg17 located in the N and C termini of TP I and other residues such as Ile11 and Cys12 were particularly

increased by the interaction with LPS. These results indicated the possibility of the structural stabilization of whole TP I containing N and C termini in complex with LPS. In the presence of LPS, the tr-NOESY spectrum showed the long range NOEs observed under the aqueous condition as well as the peaks of W2/R17. These peaks suggested that TP I in the presence of LPS adopts an antiparallel structure like that of TP I in aqueous solution.

Three-dimensional structure of TP I with or without LPS

I calculated the TP I structure in an aqueous solution by use of 110 distance constraints of NOEs (Fig. 4a). From the backbone dihedral angles of the calculated structure, TP I was suggested to adopt an antiparallel β-sheet composed of Phe4 - Cys7 and Cys12 - Arg15. The N and C termini did not converge well when the 20 lowest energy structures were superimposed (Fig. 4a). The poor convergence of the N and C termini suggested their structural flexibility. The RMSD value of the well-defined region (Cys3-Cys16) was 0.771 Å for the backbone atoms.

The LPS-bound structure of TP I was determined by using 216 Tr-NOE-driven distance constraints (Fig. 4b). The structural statistics are summarized in Table 1. The backbone dihedral angles suggested that the antiparallel β-sheet structure of TP I is composed of two strands of Cys3-Cys7 and Cys12-Cys16. TP I appeared to slightly extend its two β-strands by binding to LPS. The RMSD value of the well-defined region (Cys3-Cys16) was 0.632 Å for the backbone atoms. This RMSD value is smaller than that of the TP I structure without LPS, suggesting that the structure of TP I is stabilized by binding to LPS. In addition, the NMR structure showed that the backbone of the N and C termini is more rigid in LPS than in water. Further, TP I exhibited a twisted structure in the presence of LPS. In order to evaluate the twist quantitatively, I measured the $C3C^{\alpha}$-$C16C^{\alpha}$ -$C12C^{\alpha}$ -$C7C^{\alpha}$ dihedral angle of the twenty lowest-energy TP I structures. The dihedral angle in water was $12.0^{o} \pm 30.5^{o}$, while that in the presence of LPS was $53.4^{o} \pm 17.3^{o}$. Conformational changes in TP I

occurred via an interaction with LPS, which was consistent with the results of CD measurements; these changes included the elongation of two β-strands and structural stabilization.

Tryptophan fluorescence studies

I then investigated the interaction site between TP I and LPS by using spectroscopic techniques. To determine the local environment of W2, the intrinsic tryptophan fluorescence emission wavelength was monitored. Tryptophan fluorescence is widely used to judge the polarity of the local environment [20]. In a polar environment, tryptophan fluorescence shifts toward longer wavelength. Meanwhile, in an environment of low polarity, tryptophan fluorescence shifts toward shorter wavelength (blue shift). In the absence of LPS, the maximum wavelength of tryptophan fluorescence emission was 360 nm. The tryptophan fluorescence emission maxima of TP I showed a concentration-dependent blue shift by the additions of LPS (Fig. 5a). When the concentrations of LPS were saturated, the maximum wavelength of tryptophan fluorescence emission was 332 nm. This remarkable blue shift indicated that the tryptophan residue of TP I is incorporated into the hydrophobic environment of LPS. In order to assess the degree of solvent exposure of the tryptophan residue, florescence quenching studies were carried out for TP I in the presence or absence of LPS by using acrylamide as a quencher. Figure 5b shows Stern-Volmer plots of the tryptophan fluorescence intensity of TP I with or without LPS. The values of the Stern-Volmer constants, K_{SV} for TP I 21.7 M^{-1} in water and K_{SV} for TP I in LPS 9 M^{-1}, were estimated from the slope of the Stern-Volmer plots. As shown in Fig. 5b, TP I experienced a large quenching in its free state. This large quenching indicated an exposure of tryptophan residue to the aqueous solvent. On the other hand, the quenching of tryptophan fluorescence was limited in the presence of LPS. The limited quenching indicated a reduction in the accessibility of the tryptophan residue to acrylamide by the interaction with LPS. These

intrinsic tryptophan fluorescence studies demonstrated that the Trp2 or N-terminal residues of TP I are involved in binding to the hydrophobic region of LPS.

1D ^{1}H NMR measurement of TP I in LPS

I obtained 1D ^{1}H NMR spectra in the presence or absence of LPS to identify the residues involved in binding to LPS. Figure 6 shows a low field of the 1D ^{1}H NMR spectra. As shown in the difference spectrum in this figure, several peaks of TP I (arrows) changed their chemical shift values upon the addition of LPS evidenced by the phase changes in the difference spectrum. These peaks were assigned to the NHs of the W2, C3, and R17 residues, which are located in the N and C termini of TP I. These chemical shift changes indicated that residues located in the N and C termini of TP I are involved in binding to LPS. The suggestion that the Trp2 residue was involved in binding to LPS was consistent with the results of tryptophan fluorescence measurements and quenching studies.

1D ^{31}P NMR measurement of LPS in the presence of TP I

In order to investigate the site of the interaction between LPS and TP I, I measured 1D ^{31}P NMR spectra of LPS with or without TP I. In the presence of TP I, LPS showed two peaks, at 2.25 ppm and at 1.44 ppm (Fig. 7). The resonance at 2.25 ppm corresponded to the diphosphate linked to GlcN of LPS and the resonance at 1.44 ppm corresponded to the monophosphate of LPS [32,33]. By the addition of TP I solution, the ^{31}P resonance of LPS at 2.25 ppm was slightly shifted upfield. On the other hand, the peak intensity of the ^{31}P resonance of LPS at 1.44 ppm was significantly changed by binding to TP I. These changes of chemical shift and peak intensity suggested that the phosphate groups of LPS are in close proximity to TP I.

Complex structure of TP I and LPS

The five lowest-energy TP I structures in the LPS-bound state calculated by the distance constraints obtained from Tr-NOE were docked with LPS by the program AutoDock ver. 4.2. The detailed structure of LPS used in the docking calculation is shown in Fig. 8a. Each docking calculation produced 200 docked structures, and I analyzed the complex structures that showed negative free energy as a result of the docking calculation. In the majority of the complex structures for which the simulation-calculated Kd values were under 100 μM, the TP I lay down on the two GlcNs of LPS (Fig. 8b, c). In the complex, some basic residues appeared to form hydrogen bonds or salt bridges with phosphate groups or saccharides. The $N^{\zeta}H$ (amino group) of Lys1 was in close proximity to the phosphate groups of LPS, and the guanidyl group or amidated C terminus of Arg17 was also located close to the same phosphate groups. The guanidyl group of the Arg14 or Arg15 residue was close to the saccharides, which were located on the upper part of GlcNs. Close packing was observed not only between the basic residues and the phosphate groups or saccharides but also between aromatic residues and the hydrophobic region of LPS. The indole ring of Trp2 was located near the acyl chains, a constituent of lipid A. The aromatic ring of Phe4 was also in close proximity to the acyl chains of LPS and was approximately parallel to the plane of acyl chains. This docking model showed that cationic residues located in the N and C termini of TP I interact with phosphate groups or saccharides of LPS, whereas hydrophobic residues such as Trp2 and Phe4 in the N terminus interact with the acyl chains of LPS (Fig. 8c). The key residues of TP I for interaction with LPS revealed by this docking model are consistent with the results of Trp fluorescence studies and 1D ^{1}H NMR.

I-5 Discussion

Over the past few decades, numerous AMPs have been identified and their activities and structures investigated [6-9,34-36]. Recently, in an attempt to overcome sepsis and other diseases caused by Gram-negative bacteria, the application of AMPs to new agents has been attracting much attention. Many reports have analyzed the structures of AMPs in the presence of LPS or mimetic membrane of Gram-negative bacteria to understand the mechanism of LPS or lipid-membrane recognition in AMPs [37-39]. However, the details of the interaction between AMPs and LPS and the relationship between the mechanisms of LPS recognition and structures of AMPs have not yet been revealed.

As one of the AMPs that can bind to LPS, TP I has been intensively studied. It is well known that TP I has broad spectrum antimicrobial activity against Gram-negative and Gram-positive bacteria as well as fungi [15,40]. In water, TP I forms an antiparallel β-hairpin and amphipathic structure. Furthermore, Laederach et al. [18] revealed that the N and C termini of TP I are folded toward the turn region in the presence of DPC micelles. In contrast, Mizuguchi et al. [41] proposed that TP I adopts a straight β-hairpin structure in the presence of DPC micelles (PDB ID 1WO1). Doherty et al. [42] reported that no bending is observed in the β-strands of TP I in the lipid bilayer, and concluded that TP I is parallel to the membrane plane and immersed in the interfacial region of the membrane.

In this study, I determined the structure of TP I in its bound state with LPS by the use of Tr-NOESY (Fig. 2b, 4b). Structural analysis revealed that TP I extends its β-sheet structure and stabilizes this structure by binding to LPS. These structural properties were consistent with the results of CD measurements (Fig. 1) that suggested a slight change in the secondary structures of TP I between its free state and LPS-binding state. Intrinsic tryptophan fluorescence studies and fluorescence quenching studies suggested that Trp2 was incorporated into the hydrophobic environment of LPS (Fig. 5). 1D ^{1}H NMR and 1D

^{31}P NMR revealed that the Trp2, Cys3, and Arg17 residues of TP I are involved in binding to LPS, while the phosphate groups of LPS are involved in binding to TP I (Fig. 6, 7). The complex structure obtained by docking calculation between TP I and LPS showed that TP I lies across the two GlcNs of LPS (Fig. 8). In the complex, cationic residues such as Lys1, Arg15, and Arg17 of TP I interact with the phosphate groups or saccharides of LPS, whereas the aromatic residues Trp2 and Phe4 interact with the acyl chains of LPS. These interaction sites of TP I and LPS shown in complex structure were consistent with the results of intrinsic tryptophan fluorescence and 1D ^{1}H and ^{31}P NMR studies. By binding to LPS, TP I seems to twist its antiparallel β-sheet structure. This conformational change may occur due to the Lys1 and Arg17 residues simultaneously recognizing the same phosphate group of LPS. In other words, a twisting β-sheet structure may be important for TP I to recognize LPS. In fact, few complex structures of TP I and LPS were acquired by docking calculations using the TP I structure in aqueous solution (data not shown).

In recent years, the structure of a TP I mutant in which all four Cys residues were deleted, named CDT, was clarified in its LPS-bound state [19]. Although CDT adopts a random coil conformation in aqueous solution, it adopts a β-hairpin-like structure in the presence of LPS. The Y6-I9 of CDT makes a type II' β-turn and W2-V5 and Y10-R13 are respectively extended. Some side chains of the Arg residues of CDT interact with phosphate groups of lipid A and a hydrophobic surface composed of W2, F3, Y6, I9 and Y10 is inserted along the acyl chains of lipid A.

Comparing the TP I-LPS complex with the CDT-LPS complex, I note several similarities. First, the guanidyl groups of Arg residues located in the C terminus were important for both peptides to interact with the phosphate groups of LPS. Secondly, aromatic residues such as W2 and F4 (F3 in CDT) were inserted into the hydrophobic acyl chains of LPS. However, there were also some differences between the TP I-LPS complex and CDT-LPS complex. In the case of TP I, the side chain of K1 was in close proximity to

the phosphate group, but K1 of CDT was not involved in the interaction with the phosphate group. The side chain of R9 of TP I was not close to the phosphate group of LPS, but the side chain of R7 of CDT corresponding to R9 of TPI was in close proximity to the phosphate group of LPS. Further, the backbone and side chains of I9 (I11 in TP I) of CDT were in close proximity to LPS, while I11 of TP I seemed unlikely to be involved in binding to LPS. In addition, the peptide locations in LPS were drastically different. CDT was located at the base of the acyl chains of lipid A, while TP I lay on two glucosamine residues. These differences may suggest that TP I and CDT interact with LPS in distinct ways.

In conclusion, I revealed that binding to LPS slightly extends the two β-strands of TP I and stabilizes the whole structure of TP I. Fluorescence studies indicated that a tryptophan residue is incorporated into the hydrophobic environment of LPS. 1D ^{1}H NMR study suggested that residues located in the N and C termini of TP I were involved in the binding to LPS. 1D ^{31}P NMR measurements suggested that phosphate groups of LPS were in close proximity to TP I. Finally, I proposed the model structure of the complex of TP I with LPS by using a docking program. The calculated model structure suggested that the cationic residues of TP I interact with the phosphate groups and saccharides of LPS, whereas the hydrophobic residues interact with the acyl chains of LPS. The complex structure of TP I and LPS that I revealed in this report provides detailed structural knowledge about the binding of TP I to LPS. I hope that these findings will be fundamental to elucidating the LPS recognition system of AMPs.

I-6 References

[1] H. Nikaido, Prevention of drug access to bacterial targets: permeability barriers and active efflux, Science 264 (1994) 382-388.

[2] L. Zhang, M.G. Scott, H. Yan, L.D. Mayer, R.E. Hancock, Interaction of polyphemusin I and structural analogs with bacterial membranes, lipopolysaccharide, and lipid monolayers, Biochemistry 39 (2000) 14504-14514.

[3] J. Cohen, The immunopathogenesis of sepsis, Nature 420 (2002) 885-891.

[4] A. Bhunia, A. Ramamoorthy, S. Bhattacharjya, Helical hairpin structure of a potent antimicrobial peptide MSI-594 in lipopolysaccharide micelles by NMR spectroscopy, Chemistry 15 (2009) 2036-2040.

[5] J. Mares, S. Kumaran, M. Gobbo, O. Zerbe, Interactions of lipopolysaccharide and polymyxin studied by NMR spectroscopy, J. Biol. Chem. 284 (2009) 11498-11506.

[6] D. Sipos, M. Andersson, A. Ehrenberg, The structure of the mammalian antibacterial peptide cecropin P1 in solution, determined by proton-NMR, Eur. J. Biochem. 209 (1992) 163-169.

[7] N. Mandard, P. Sodano, H. Labbe, J.M. Bonmatin, P. Bulet, C. Hetru, M. Ptak, F. Vovelle, Solution structure of thanatin, a potent bactericidal and fungicidal insect peptide, determined from proton two-dimensional nuclear magnetic resonance data, Eur. J. Biochem. 256 (1998) 404-410.

[8] N. Mandard, P. Bulet, A. Caille, S. Daffre, F. Vovelle, The solution structure of gomesin, an antimicrobial cysteine-rich peptide from the spider, Eur. J. Biochem. 269 (2002) 1190-1198.

[9] W. Gong, J. Wang, Z. Chen, B. Xia, G. Lu, Solution structure of LCl, a novel antimicrobial peptide from *Bacillus subtilis*, Biochemistry 50 (2011) 3621-3627.

[10] Y. Huang, J. Huang, Y. Chen, Alpha-helical cationic antimicrobial peptides:

relationships of structure and function, Protein Cell 1 (2010) 143-152.

[11] M. Zasloff, Antimicrobial peptides of multicellular organisms, Nature 415 (2002) 389-395.

[12] Q.P. Lin, L.F. Zhou, N.N. Li, Y.Q. Chen, B.C. Li, Y.F. Cai, S.Q. Zhang, Lipopolysaccharide neutralization by the antibacterial peptide CM4, Eur. J. Pharmacol 596 (2008) 160-165.

[13] A. Bhunia, H. Mohanram, S. Bhattacharjya, Lipopolysaccharide bound structures of the active fragments of fowlicidin-1, a cathelicidin family of antimicrobial and antiendotoxic peptide from chicken, determined by transferred nuclear Overhauser effect spectroscopy, Biopolymers 92 (2009) 9-22.

[14] A. Bhunia, P.N. Domadia, J. Torres, K.J. Hallock, A. Ramamoorthy, S. Bhattacharjya, NMR structure of pardaxin, a pore-forming antimicrobial peptide, in lipopolysaccharide micelles: mechanism of outer membrane permeabilization, J. Biol. Chem. 285 (2010) 3883-3895.

[15] T. Nakamura, H. Furunaka, T. Miyata, F. Tokunaga, T. Muta, S. Iwanaga, M. Niwa, T. Takao, Y. Shimonishi, Tachyplesin, a class of antimicrobial peptide from the hemocytes of the horseshoe crab (*Tachypleus tridentatus*). Isolation and chemical structure, J. Biol. Chem. 263 (1988) 16709-16713.

[16] Y. Hirakura, S. Kobayashi, K. Matsuzaki, Specific interactions of the antimicrobial peptide cyclic beta-sheet tachyplesin I with lipopolysaccharides, Biochim. Biophys. Acta 1562 (2002) 32-36.

[17] K. Kawano, T. Yoneya, T. Miyata, K. Yoshikawa, F. Tokunaga, Y. Terada, S. Iwanaga, Antimicrobial peptide, tachyplesin I, isolated from hemocytes of the horseshoe crab (*Tachypleus tridentatus*). NMR determination of the beta-sheet structure, J. Biol. Chem. 265 (1990) 15365-15367.

[18] A. Laederach, A.H. Andreotti, D.B. Fulton, Solution and micelle-bound structures of

tachyplesin I and its active aromatic linear derivatives, Biochemistry 41 (2002) 12359-12368.

[19] R. Saravanan, H. Mohanram, M. Joshi, P.N. Domadia, J. Torres, C. Ruedl, S. Bhattacharjya, Structure, activity and interactions of the cysteine deleted analog of tachyplesin-1 with lipopolysaccharide micelle: Mechanistic insights into outer-membrane permeabilization and endotoxin neutralization, Biochim. Biophys. Acta 1818 (2012) 1613-1624.

[20] J.P. Powers, A. Rozek, R.E. Hancock, Structure-activity relationships for the beta-hairpin cationic antimicrobial peptide polyphemusin I, Biochim. Biophys. Acta 1698 (2004) 239-250.

[21] F. Delaglio, S. Grzesiek, G.W. Vuister, G. Zhu, J. Pfeifer, A. Bax, NMRPipe: a multidimensional spectral processing system based on UNIX pipes, J. Biomol. NMR 6 (1995) 277-293.

[22] T.D. Goddard, D.G. Kneller, SPARKY 3, University of California, San Francisco, 2006

[23] L. Braunschweiler, R.R. Ernst, Coherence transfer by isotropic mixing: Application to proton correlation spectroscopy, J. Magn. Reson. 53 (1983) 521-528.

[24] C.B. Post, Exchange-transferred NOE spectroscopy and bound ligand structure determination, Curr. Opin. Struct. Biol. 13 (2003) 581-588.

[25] C.D. Schwieters, J.J. Kuszewski, N. Tjandra, G.M. Clore, The Xplor-NIH NMR molecular structure determination package, J. Magn. Reson. 160 (2003) 65-73.

[26] C.D. Schwieters, J.J. Kuszewski, G.M. Clore, Using Xplor-NIH for NMR molecular structure determination, Prog. Nucl. Magn. Reson. Spectrosc. 48 (2006) 47-62.

[27] R.A. Laskowski, J.A. Rullmannn, M.W. MacArthur, R. Kaptein, J.M. Thornton, AQUA and PROCHECK-NMR: programs for checking the quality of protein structures solved by NMR, J.Biomol. NMR 8 (1996) 477-486.

[28] W.L. DeLano, The PyMOL molecular graphics system, Version 1.6.0.0 Schrödinger,

LLC, 2013.

[29] G.M. Morris, R. Huey, W. Lindstrom, M.F. Sanner, R.K. Belew, D.S. Goodsell, A.J. Olson, AutoDock4 and AutoDockTools4: Automated docking with selective receptor flexibility, J. Comput. Chem. 30 (2009) 2785-2791.

[30] A.D. Ferguson, W. Welte, E. Hofmann, B. Lindner, O. Holst, J.W. Coulton, K. Diederichs, A conserved structural motif for lipopolysaccharide recognition by procaryotic and eucaryotic proteins, Structure 8 (2000) 585-592.

[31] L. Yu, M. Tan, B. Ho, J.L. Ding, T. Wohland, Determination of critical micelle concentrations and aggregation numbers by fluorescence correlation spectroscopy: aggregation of a lipopolysaccharide, Anal. Chem. Acta 556 (2006) 216-225.

[32] S.M. Strain, S.W. Fesik, I.M. Armitage, Structure and metal-binding properties of lipopolysaccharides from heptoseless mutants of *Escherichia coli* studied by ^{13}C and ^{31}P nuclear magnetic resonance, J. Biol. Chem. 258 (1983) 13466-13477.

[33] S. Müller-Loennies, O. Holst, B. Lindner, H. Brade, Isolation and structural analysis of phosphorylated oligosaccharides obtained from *Escherichia coli* J-5 lipopolysaccharide, Eur. J. Biochem. 260 (1999) 235-249.

[34] D. Marion, M. Zasloff, A. Bax, A two-dimensional NMR study of the antimicrobial peptide magainin 2, FEBS Lett. 227 (1988) 21-26.

[35] A. Aumelas, M. Mangoni, C. Roumestand, L. Chiche, E. Despaux, G. Grassy, B. Calas, A. Chavanieu, Synthesis and solution structure of the antimicrobial peptide protegrin-1, Eur. J. Biochem. 237 (1996) 575-583.

[36] K. Matsuzaki, Why and how are peptide-lipid interactions utilized for self-defense? Magainins and tachyplesins as archetypes, Biochim. Biophys. Acta 1462 (1999) 1-10.

[37] B.F. Tack, M.V. Sawai, W.R. Kearney, A.D. Robertson, M.A. Sherman, W. Wang, T. Hong, L.M. Boo, H. Wu, A.J. Waring, R.I. Lehrer, SMAP-29 has two LPS-binding sites and a central hinge, Eur. J. Biochem. 269 (2002) 1181-1189.

[38] F. Porcelli, R. Verardi, L. Shi, K.A. Henzler-Wildman, A. Ramamoorthy, G. Veglia, NMR structure of the cathelicidin-derived human antimicrobial peptide LL-37 in dodecylphosphocholine micelles, Biochemistry 47 (2008) 5565-5572.

[39] T.J. Park, J.S. Kim, H.C. Ahn, Y. Kim, Solution and solid-state NMR structural studies of antimicrobial peptides LPcin-I and LPcin-II, Biophys. J. 101 (2011) 1193-1201.

[40] A.G. Rao, Conformation and antimicrobial activity of linear derivatives of tachyplesin lacking disulfide bonds, Arch. Biochem. Biophys. 361 (1999) 127-134.

[41] M. Mizuguchi, S. Kamata, S. Kawabata, K. Kawano, Structure of horseshoe crab antimicrobial peptide, tachyplesin I in dodecylphosphocholine micelles, Pept. Sci. 2002 (2003) 281-282.

[42] T. Doherty, A.J. Waring, M. Hong, Membrane-bound conformation and topology of the antimicrobial peptide tachyplesin I by solid-state NMR, Biochemistry 45 (2006) 13323-13330.

Table 1. Summary of the structural statistics for the 20 lowest energy structures of TP I in its free and LPS-bound state.

	free	+LPS
Distance restraints		
Intra-residue	65	101
Sequential	34	69
Medium-range	2	13
Long-range	9	33
Total	110	216
Angular restraints	15	13
Deviation from mean structure (only for the well-defined region C3-C16)		
Backbone (Å)	0.771	0.632
Ramachandran plot analysis		
% Residues in the most favorable regions	65.7	78.9
% Residues in additionally allowed regions	29.3	20.0
% Residues in generously allowed regions	5.0	1.1
% Residues in disallowed regions	0.0	0.0

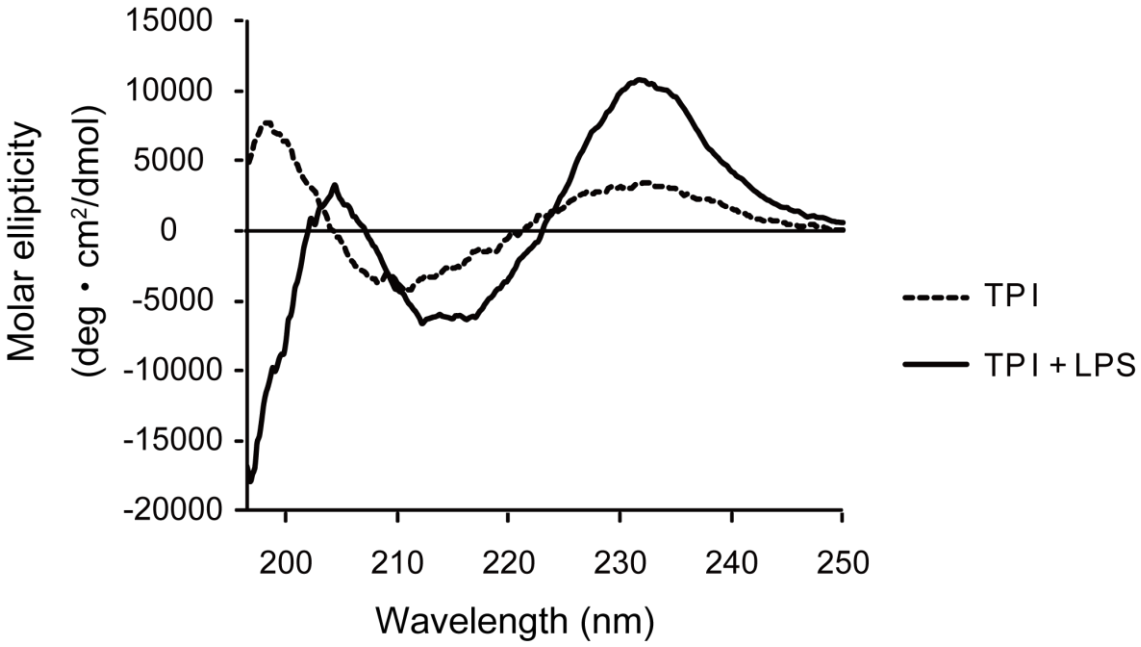

Figure 1. CD spectra of TP I in the absence (dotted lines) and presence of LPS (solid lines). The concentrations of TP I and LPS were 30 μM and 72 μM in 10 mM sodium phosphate buffer (pH7.4), respectively. Measurements were carried out at 25 ºC.

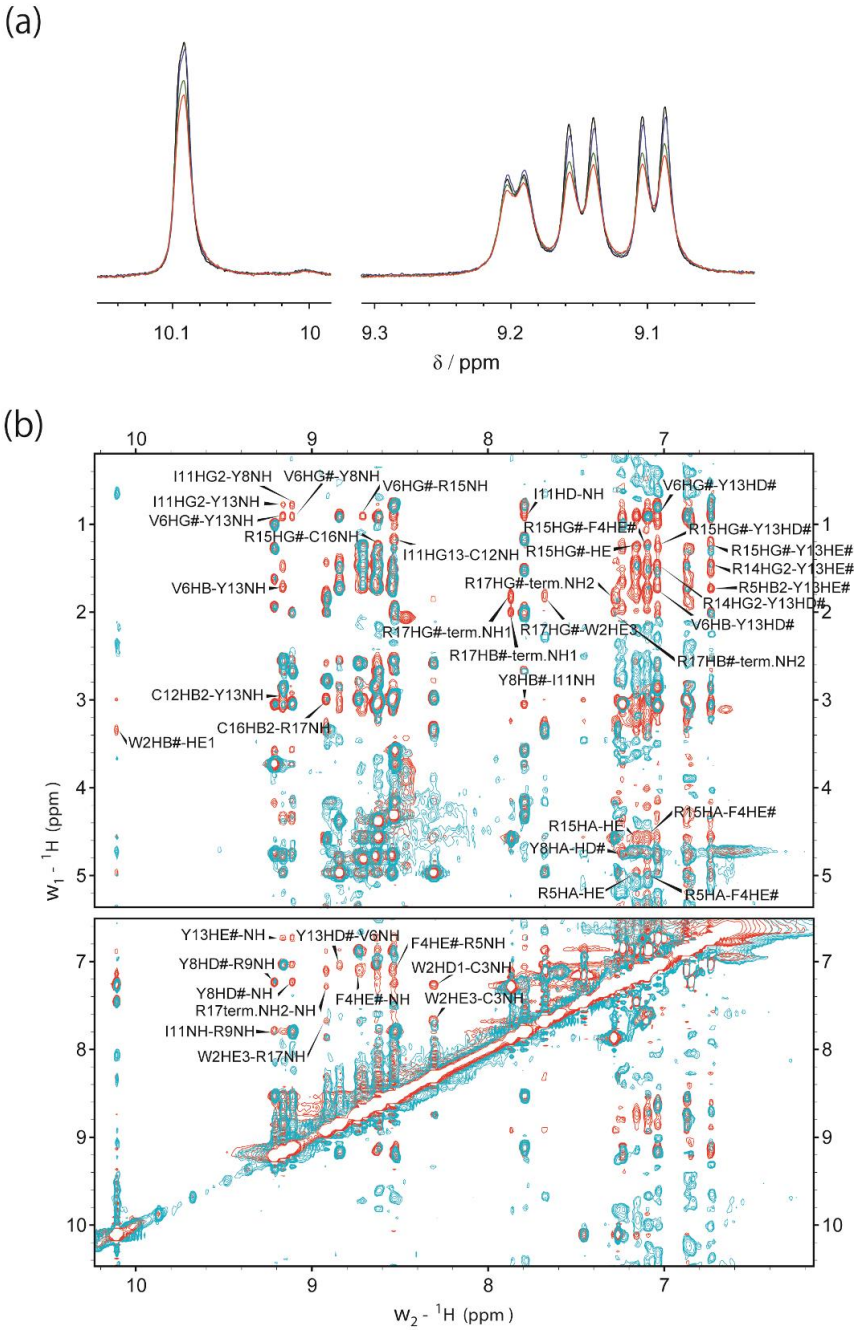

Figure 2. (a) The line-broadening by the addition of LPS to TP I solution. The TP I concentration was 750 μM and the LPS concentration was 0 (black), 20 (blue), 35 (green), or 50 μM (red) in 10% D_2O at pH 3.8. These spectra were measured at 35 ºC. (b) Superimposition of the NOESY spectrum of TP I in water and the Tr-NOESY spectrum of TP I containing LPS. Red-colored peaks were observed in the measurement of Tr-NOESY and blue-colored peaks were obtained by the measurement of NOESY. Assigned peaks were observed only in the presence of LPS.

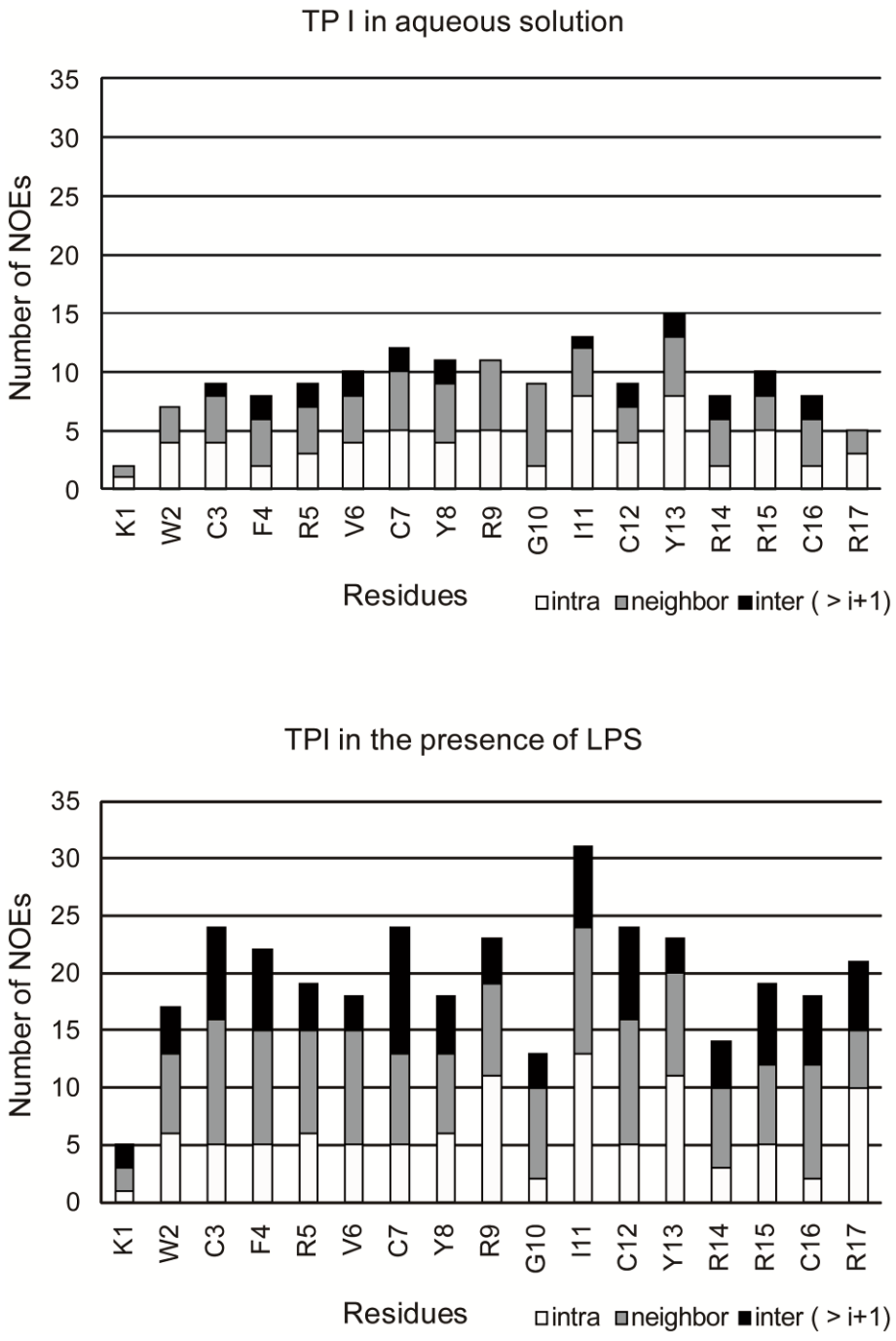

Figure 3. Histogram showing the number of NOEs of TP I as a function of residues with or without LPS.

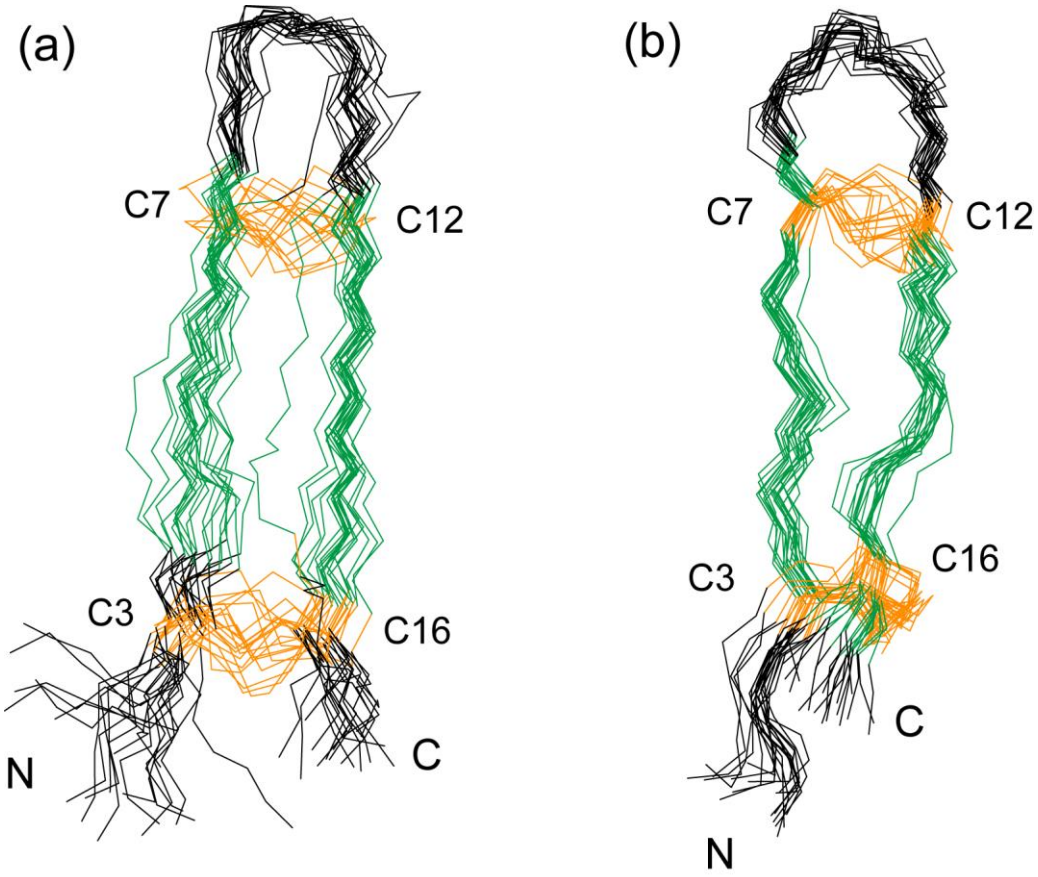

Figure 4. Superimposition of the 20 lowest-energy structures of TP I in water (a) and in the presence of LPS (b). β-strands are shown in green and disulfide bonds are shown in orange.

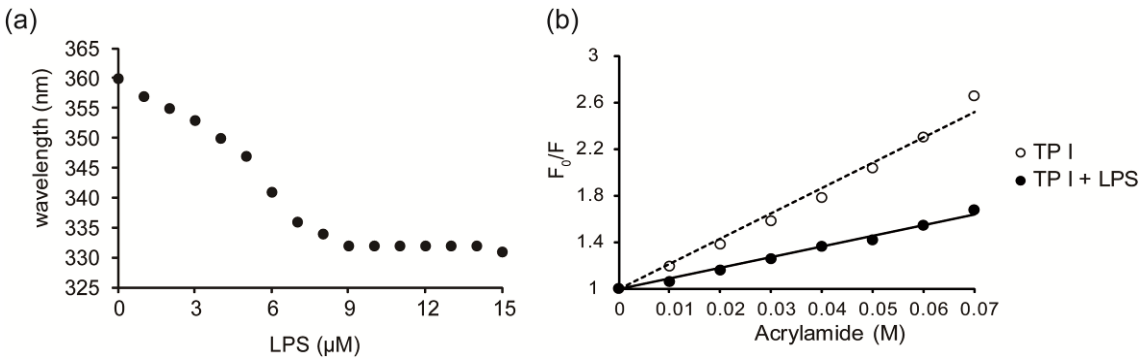

Figure 5. (a) Plot showing changes in maximal emission wavelength of the intrinsic tryptophan fluorescence of TP I, as a function of increasing concentrations of LPS. TP I was dissolved in 10 mM sodium phosphate buffer (pH7.4) at a final concentration of 5 μM. (b) Fluorescence quenching of TP I by acrylamide in 10 mM sodium phosphate buffer at pH 7.4 with or without LPS. The concentrations of TP I and LPS were 5 μM and 12 μM, respectively.

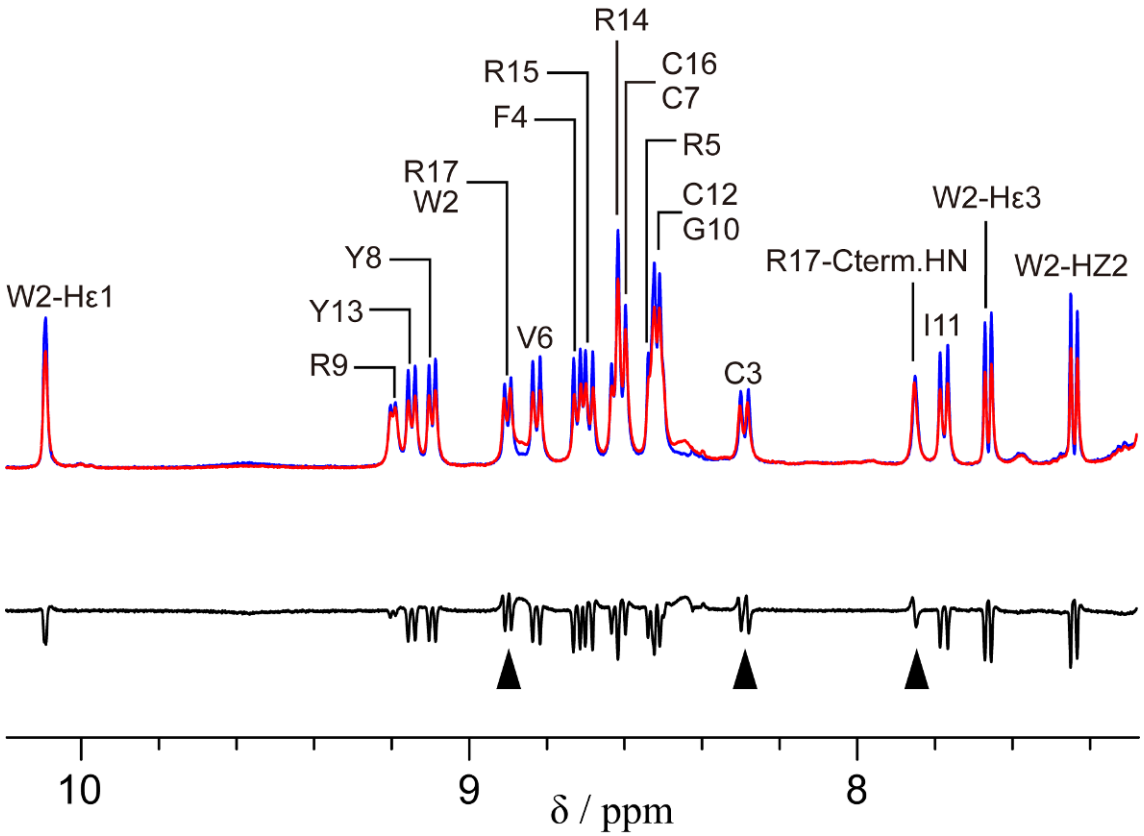

Figure 6. Low-field resonances of 1D ^{1}H NMR spectra of TP I with LPS (red) or without LPS (blue). The TP I and LPS concentrations were respectively 750 μM and 50 μM in 10% D_2O at pH 3.8. These spectra were measured at 35 ºC. The black spectrum represents the difference between the two spectra. Arrows indicate chemical shift changes of TP I by the addition of LPS.

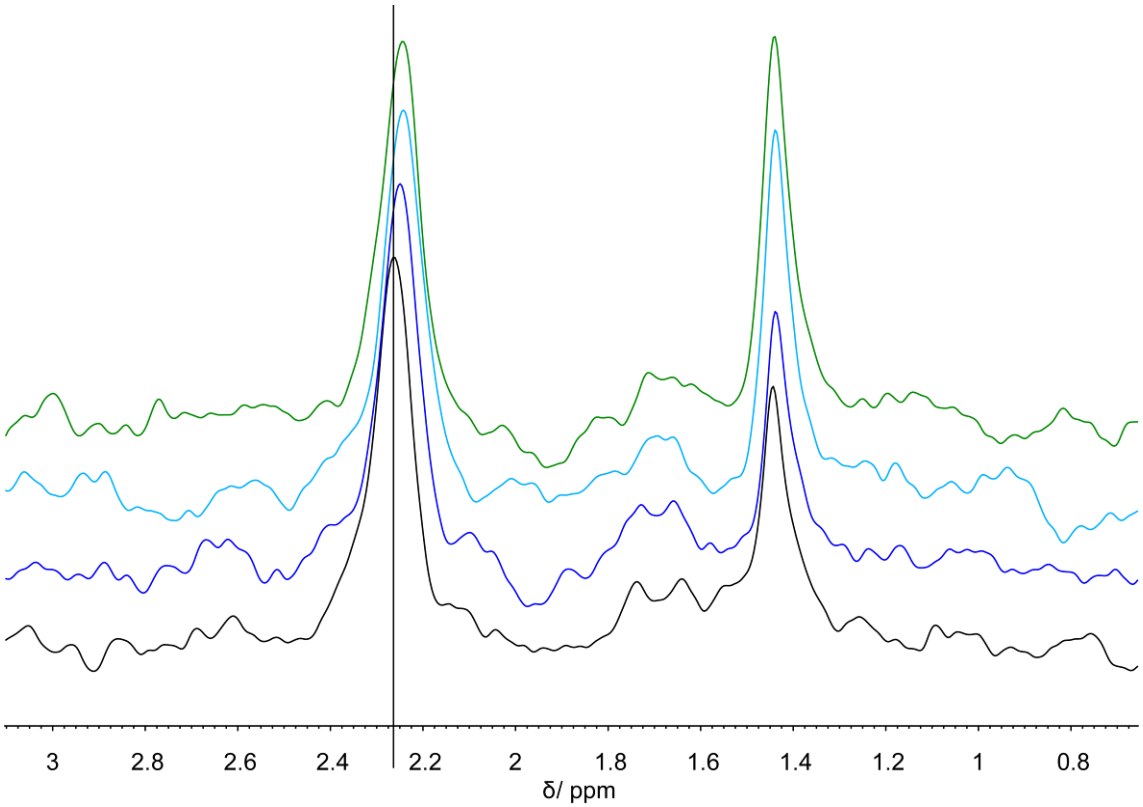

Figure 7. 1D ^{31}P NMR spectra of LPS with various concentrations of TP I measured at 35 ºC. LPS was dissolved in 10% D_2O, pH 3.8, at a final concentration of 400 μM. The spectra displayed in black, purple, blue and green indicate LPS:TP I molar ratios of 1:0, 1:0.5, 1:1, and 1:1.5, respectively.

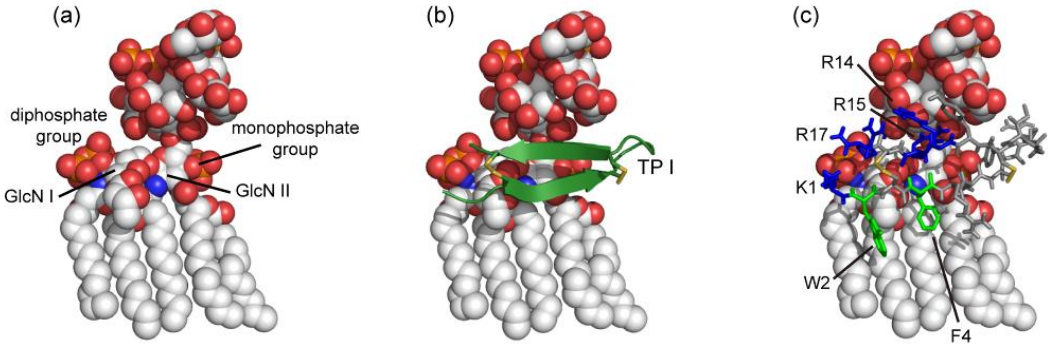

Figure 8. (a) LPS structure used in the docking calculation. GlcN: 3-deoxy-D-glucosamine. (b) The complex structure of TP I and LPS. TP I is shown as a cartoon and (c) sticks. The docking model was calculated by using the structure of TP I in its LPS-bound state and the crystal structure of LPS (PDB ID 1QFG). Key cationic residues of TP I (K1, R14, R15 and R17) for binding to LPS are shown in blue, and aromatic residues (W2 and F4) interacting with the acyl chains of LPS are shown in green.

Part II

Chitin-binding site of tachyplesin I, an antimicrobial peptide of horseshoe crab

II-1 Abstract

Chitin, a linear β-1,4-linked polymer of N-acetylglucosamine, is an essential component of fungal cell walls. Some antimicrobial peptides (AMPs) are thought to exert their antifungal activity by binding to chitin, but the details of the interaction between them are less well studied. To gain better understanding of the chitin-binding ability of AMPs, I determined the chitin-binding site of tachyplesin I (TP I), an antimicrobial peptide isolated from horseshoe crab.

One-dimensional ^{1}H NMR study indicated that the four residues, F4, R9, Y13 and R17, of TP I are involved in binding to hexa-N-acetyl-chitiohexaose, the largest soluble derivative of chitin. I investigated the importance of these residues for chitin-binding by the use of TP I mutants. From the results of the chitin-binding assay of TP I and its mutants, it was confirmed that TP I can strongly bind to chitin. Meanwhile, all mutants reduced the chitin-binding ability. The replacement of F4 and Y13 especially attenuated the chitin-binding ability, and the mutant in which all four residues were replaced with Ala exhibited a marked reduction in chitin-binding ability. These results indicated that aromatic F4 and Y13 are the most important residues for the binding of TP I to chitin, while cationic R9 and R17 are only secondarily involved in this binding.

II-2 Introduction

Fungi are generally known as a harmless commensal in humans, but they can cause serious infection when the host becomes debilitated or immunocompromised. Indeed, these opportunistic invasive fungal infections are a major cause of morbidity and mortality in immunocompromised patients [1-3].

To overcome fungal infections, many antifungal drugs have been developed, such as polyenes [4], azoles [5] and echinocandins [6]. But lately, fungi resistant to such drugs have begun to emerge and to become a medical problem [7, 8]. Because it is generally considered much more difficult for microbes to develop resistance to antimicrobial peptides (AMPs) than to antibiotics [9], AMPs have recently received increased attention in the field of drug discovery [10].

AMPs are ubiquitously found in living organisms [11-14] and are important components of the innate immune response. Most AMPs exhibit a wide spectrum of antimicrobial activity against Gram-negative and Gram-positive bacteria as well as fungi [15]. In the case of AMPs which exert antifungal activity, some of them are thought to target chitin, an essential component of the cell wall of fungi [16, 17]. Thus an understanding of the chitin recognition mechanism of AMPs is important to reveal the mechanism of antifungal activity. However, there have been few reports about the chitin-binding ability of AMPs and structural information of AMPs in their chitin-binding state.

Tachyplesin I (TP I) is a 17-residue antimicrobial peptide found in the hemocytes of the horseshoe crab, *Tachypleus tridentatus* [18]. In aqueous solution, TP I adopts an anti-parallel β-sheet structure stabilized by two disulfide bonds [19]. TP I exhibits strong activity against Gram-negative and -positive bacteria as well as fungi [18, 20]. The chitin-binding ability of TP I has been established [21], but the details of the interaction between TP I and chitin have remained unclear.

To clarify the details of the interaction between TP I and chitin, I investigated the site of binding of chitin by TP I using ^{1}H nuclear magnetic resonance (NMR) measurements. Based on the results, I prepared TP I mutants and identified the key residues for the chitin-binding ability of TP I.

II-3 Materials and Methods

Reagents

Chitin was obtained from Funakoshi Co., Ltd. (Tokyo) and hexa-N-acetylchitohexaose was supplied by Seikagaku Corp. (Tokyo); both were used in all experiments without any purification.

All peptides used in this study were synthesized by Fmoc solid phase chemistry (Sigma Life Science, Sigma-Aldrich Corp., St. Louis, MO). Based on the protocols of Powers *et al*. [22], these peptides were oxidized to form disulfide bonds before use. For example, TP I (KWCFRVCYRGICYRRCR-NH2) was dissolved in 20 mM Tris-HCl buffer (pH 8.0) containing 20% DMSO and shaken for more than 24 hours at room temperature to promote disulfide bond formation. The correctly folded TP I (C3-C16 and C7-C12) was then separated and purified by reverse-phase HPLC. Two disulfide bonds of the purified peptide were confirmed by MALDI-TOF mass spectroscopy through an observed 4 mass unit difference between the reduced and oxidized forms of TP I. Oxidized TP I solution was lyophilized and stored at -80ºC. I followed the same procedure for the other peptides.

NMR measurements

All NMR spectra were recorded either on a JEOL ECA 600 MHz spectrometer or a BRUKER DMX 600 MHz equipped with a cryo-probe. Data were processed using NMRPipe 4.1 and NMRDraw 2.3 [23] and analyzed using Sparky 3.113 software [24]. One-dimensional ^{1}H NMR experiments were performed at 308 K with a TP I concentration of 1 mM in 90% H_2O / 10% D_2O solution with or without 9 mM hexa-N-acetyl-chitohexaose at pH 3.8. The one-dimensional ^{1}H NMR spectrum of TP(F4A R9A Y13A R17A) was measured at 308 K. The concentration of peptide was 240 μM in

90% H_2O / 10% D_2O and the pH was adjusted to 3.8.

Two-dimensional TOCSY [25] spectra of peptides with or without hexa-N-acetyl-chitohexaose were acquired in an aqueous solution containing 10% D_2O at pH 3.8 with 1 mM TP I and 9 mM hexa-N-acetyl-chitohexaose and mixing times of 90 ms at 308K.

Chitin-binding assay

The chitin-binding ability of peptides was assayed basically as described in the report of Kawabata *et al*. [26]. Briefly, 5 mg chitin was added to 50 mM Tris-HCl (pH8.0) containing 0.1 M NaCl and 0.01% Tween 20. The solution containing chitin was added to a spin column and centrifuged for 1 minute at 15,000 rpm. Peptide solution (10 μM) was then added to the same spin column, and the mixture was incubated at room temperature for 10 minutes. After incubation, the spin column was centrifuged for 1 minute at 15,000 rpm. The flow-through solution was reserved for reverse-phase HPLC. The spin column was then washed using 50 mM Tris-HCl (pH8.0) containing 1 M NaCl and 0.01% Tween 20. Then 10% acetic acid containing 0.01% Tween 20 was added to the spin column, and the solution was centrifuged for 1 minute at 15,000 rpm. After centrifugation, the eluted solution was reserved. Reverse-phase HPLC was then performed to check the amounts of peptides contained in the flow-through solution and the 10% acetic acid-eluted solution.

II-4 Results

Chemical shift perturbation experiment

To identify residues involved in the binding of TP I to chitin, I obtained 1D ^{1}H NMR spectra of TP I in the presence or absence of hexa-N-acetyl-chitohexaose, the largest soluble derivative of chitin. Figure 1a shows a low field of the 1D ^{1}H NMR spectra. As can be seen, some peaks of HN of TP I changed their chemical shift value upon the addition of hexa-N-acetyl-chitohexaose. Chemical shift changes were also clearly evident in the TOCSY spectra of TP I with or without hexa-N-acetyl-chitohexaose (Fig. 1b). These peaks were assigned to HN of F4, R9, Y13, and R17 of TP I. These results indicated that F4, R9, Y13 and R17 residues of TP I may have the ability to interact with hexa-N-acetyl-chitohexaose.

Chitin-binding assay of TP I and its mutants

In order to investigate whether the F4, R9, Y13 and R17 residues of TP I are important for the binding to chitin, I prepared TP I mutants in which these residues were replaced with Ala and then performed a chitin-binding assay. The sequences of the TP I mutants are summarized in Table **1**. I calculated the proportion of peptides in the solution eluted by 10% acetic acid (Fig. **2**). The sum total of peptides in the flow-through solution and eluted solution was defined as 100%. If the peptides had a low binding ability against chitin, then they would be expected to be present in the flow-through solution but not in the 10% acetic acid-eluted sample. On the other hands, peptides with high binding ability against chitin would not be present in the flow-through solution, but would be eluted by 10% acetic acid. As shown in Fig. **2**, most of the TP I was observed in the sample eluted by 10% acetic acid. This clearly suggested that TP I binds tightly to chitin.

Next, a chitin-binding assay was performed using the single amino acid-substitution

mutants TP(F4A), TP(R9A), TP(Y13A) and TP(R17A) to investigate the effect of each residue on the chitin-binding ability of TP I. As shown in Fig. **2**, all single amino acid-substitution mutants were moderately present in the 10% acetic acid-eluted sample. These results suggested that the chitin-binding ability of these peptides is lower than that of TP I.

As can be seen in Fig. **2**, the proportions of TP(F4A) and TP(Y13A) were lower than those of TP(R9A) and TP(R17A) in the 10% acetic acid-eluted solution. This suggests that the chitin-binding ability of TP(F4A) and TP(Y13A) is lower than that of TP(R9A) and TP(R17A).

I further prepared the double amino acid-substitution mutants TP(F4A Y13A) and TP(R9 R17A). Figure **2** shows that TP(R9A R17A) was moderately present in the 10% acetic acid-eluted sample. The proportion of TP(R9A R17A) in the eluted solution was comparable to the proportion of TP(R9A). This result indicates that TP(R9A R17A) has the same degree of chitin-binding ability as TP(R9A). Meanwhile, a small amount of TP(F4A Y13A) was detected in the 10% acetic acid-eluted sample. This clearly showed that the chitin-binding ability of TP(F4A Y13A) is weakened dramatically compared with that of TP I because of the replacement of two aromatic residues with Ala.

Finally, I investigated the chitin-binding ability of TP(F4A R9A Y13A R17A), a TP I mutant in which F4, R9, Y13 and R17 are replaced with Ala. A small amount of peptide was observed in the sample eluted by 10% acetic acid. This result suggested that TP I mostly lost its chitin-binding ability by the replacement of F4, P9, Y13 and R17 with Ala, and that these residues are essential for the binding to chitin.

NMR measurement of TP(F4A R9A Y13A R17A)

I measured the NMR spectrum of TP(F4A R9A Y13A R17A) to investigate whether this peptide adopts a native-like secondary conformation. Figure **3** shows low-field of the

1D ^{1}H NMR spectra of TP(C3A C7A C12A C16A), TP I and TP(F4A R9A Y13A R17A). TP(C3A C7A C12A C16A) is a TP I mutant in which all Cys residues are replaced with Ala. By the deletion of two disulfide bonds, TP(C3A C7A C12A C16A) becomes unstructured in water [27]. Using the NMR spectra of the amide proton region of TP(C3A C7A C12A C16A) and TP I as a reference, I find that TP(F4A R9A Y13A R17A) shows good chemical shift dispersion in the amide region. This indicates that TP(F4A R9A Y13A R17A) adopts a well-defined structure.

II-5 discussion

AMPs have received increased attention in the field of drug discovery because of their wide spectrum of antimicrobial activity and the low probability of microbes acquiring resistance to them. In order to develop AMPs as novel antimicrobial agents, their structures and functions have been intensively studied in recent years [12, 28-31]. AMPs found in the hemocytes of horseshoe crab have a wide spectrum of antimicrobial activity against Gram-negative and -positive bacteria and fungi. All of the AMPs derived from horseshoe crab are known to have chitin-binding ability [26, 32, 33]. Although TP I, one of the AMPs derived from horseshoe crab, is already known to bind to chitin [21], the details of the interaction between TP I and chitin have remained unclear.

In this study, I identified the key residues for the chitin-binding ability of TP I. From the superimposition of the 1D ^{1}H NMR spectra of TP I with or without hexa-N-acetyl-chitohexaose, it was clearly confirmed that the HN chemical shifts of F4, R9, Y13, and R17 were changed by the addition of hexa-N-acetyl-chitohexaose compared with the other HN chemical shifts (Fig. **1**). Furthermore, I checked the chemical shifts of the side chains of aromatic residues. I found that the chemical shifts of the side chains of F4 and Y13 were changed in the presence of hexa-N-acetyl-chitohexaose, while the side chains of the other aromatic residues W2 and Y8 were not changed. In particular, C$^{\delta}$H of Y13 showed a relatively large change of chemical shift (data not shown). These NMR studies indicated that the F4, R9, Y13 and R17 residues of TP I have the potential to interact with hexa-N-acetyl-chitohexaose. Then, a chitin-binding assay was performed using TP I and its mutants to investigate the effect of the four residues on the chitin-binding ability. All single amino acid-substitution mutants showed lower chitin-binding ability than that of TP I. The chitin-binding abilities of TP(F4A) and TP(Y13A) were lower than those of TP(R9A) and TP(R17A). These results indicated that the aromatic F4 and Y13 residues are more

important than cationic residues R9 and R17 for the binding to chitin. The double amino acid-substitution mutants also showed low chitin-binding ability. TP(R9A R17A) showed the same degree of chitin-binding ability as TP(R9A). TP(F4A Y13A) exhibited lower chitin-binding ability than TP(R9A R17A) and all single amino acid-substitution mutants. These results also suggested that the aromatic residues F4 and Y13 play an important role in the chitin-binding. TP(F4A R9A Y13A R17A) exhibited dramatically-low chitin-binding ability. This result indicated that the F4, R9, Y13 and R17 residues are essential for the binding of TP I to chitin. In the structure of TP I, the side chains of these four residues are in the same plane of the β-sheet (Fig. **4**). One surface formed by these four residues may recognize chitin. However, in the 1D ^{1}H NMR spectrum of TP I, the chemical shifts of the side chain of aromatic residue Y8 were not changed by the addition of hexa-N-acetyl-chitohexaose, even though F4, Y8 and Y13 were located on the same plane of the β-sheet structure. This may suggest that the local structure formed by F4 and Y13 is important for chitin-binding. R9 and R17 are far from the local region formed by F4 and Y13. Thus R9 and R17 are not involved in the formation of the local region and may be involved in chitin-binding secondarily.

Finally, I measured the 1D ^{1}H NMR spectrum of TP(F4A R9A Y13A R17A) to predict the conformation. The good chemical shift dispersion in the amide region indicated the well-defined structure of TP(F4A R9A Y13A R17A). In other words, TP(F4A R9A Y13A R17A) hardly bound to chitin although it adopted a native-like secondary structure. This also suggested that replacement of the four residues did not disturb the structure of TP I. Thus all of the single and double amino acid-substitution mutants also should retain the secondary structure. Therefore, the results of the chitin-binding assay were considered to reflect the effect of side chains.

Hevein is a typical chitin-binding protein derived from the rubber tree *hevea brasiliensis* [34]. From NMR studies, it was revealed that the aromatic residues Trp21,

Trp23 and Tyr30 are important for binding to N-acetyl-glucosamine oligosaccharides [35-38]. The authors of these studies proposed that the side chains of the aromatic residues stabilize the position of the carbohydrate rings through the hydrogen bonds and stacking interaction. Tachycitin and tachystatin A and B are antimicrobial peptides of horseshoe crab and are known to exhibit antifungal activity [26, 33]. All of them can bind to chitin. Although the key residues of these peptides for binding to chitin have not been confirmed experimentally, they have been predicted by reference to the structure of the chitin-binding site of hevein [39-41]. Some of the key residues of these peptides for binding to chitin are aromatic. The result that aromatic residues of TP I are important to bind to chitin is consistent with the studies of the protein and peptides described above. The side chains of F4 and Y13 of TP I may also be essential for the binding to chitin through the hydrogen bonds and stacking interaction.

To my knowledge, TP I is the shortest antimicrobial peptide that exhibits chitin-binding activity. My findings in this study should help to clarify the mechanism of chitin-recognition of AMPs and to elucidate the relationship between antifungal activity and chitin-binding activity.

II-6 References

[1] T.J. Walsh, A.H. Groll, Emerging fungal pathogens: evolving challenges to immunocompromised patients for the twenty-first century, Transpl. Infect. Dis. 1 (1999) 247-261.

[2] S. Ascioglu, J.H. Rex, B. de Pauw, J.E. Bennett, J. Bille, F. Crokaert, D.W. Denning, J.P. Donnelly, J.E. Edwards, Z. Erjavec, D. Fiere, O. Lortholary, J. Maertens, J.F. Meis, T.F. Patterson, J. Ritter, D. Selleslag, P.M. Shah, D.A. Stevens, T.J. Walsh; Invasive Fungal Infections Cooperative Group of the European Organization for Research and Treatment of Cancer; Mycoses Study Group of the National Institute of Allergy and Infectious Diseases, Defining opportunistic invasive fungal infections in immunocompromised patients with cancer and hematopoietic stem cell transplants: An international consensus, Clin. Infect. Dis. 34 (2002) 7-14.

[3] M.F. Cheng, Y.L. Yang, T.J. Yao, C.Y. Lin, J.S. Liu, R.B. Tang, K.W. Yu, Y.H. Fan, K.S. Hsieh, M. Ho, H.J. Lo, Risk factors for fatal candidemia caused by *candida albicans* and non-albicans *Candida* species, BMC Infect. Dis. 5 (2005) 22.

[4] L. Ostrosky-Zeichner, K.A. Marr, J.H. Rex, S.H. Cohen, Amphotericin B: time for a new “gold standard”, Clin. Infect. Dis. 37 (2003) 415-425.

[5] F.C. Odds, A.J. Brown, N.A. Gow, Antifungal agents: mechanisms of action, Trends Microbiol. 11 (2003) 272-279.

[6] J.M. Balkovec, D.L. Hughes, P.S. Masurekar, C.A. Sable, R.E. Schwartz, S.B. Singh, Discovery and development of first in class antifungal caspofungin (CANCIDAS®)-A case study, Nat. Prod. Rep. 31 (2014) 15-34.

[7] C. Spampinato, D. Leonardi, *Candida* infections, causes, targets, and resistance mechanisms: Traditional and alternative antifungal agents, Biomed. Res. Int. 2013 (2013) 204237.

[8] A. Srinivasan. J.L. Lopez-Ribot, A.K. Ramasubramanian, Overcoming antifungal resistance, Drug Discov. Today Technol. 11 (2014) 65-71.

[9] M. Zasloff, Antimicrobial peptides of multicellular organisms, Nature 415 (2002) 389-395.

[10] R.E. Hancock, Peptide antibiotics, Lancet 349 (1997) 418-422.

[11] D. Sipos, M. Andersson, A. Ehrenberg, The structure of the mammalian antibacterial peptide cecropin P1 in solution, determined by proton-NMR, Eur. J. Biochem. 209 (1992) 163-169.

[12] N. Mandard, P. Sodano, H. Labbe, J.M. Bonmatin, P. Bulet, C. Hetru, M. Ptak, F. Vovelle, Solution structure of thanatin, a potent bactericidal and fungicidal insect peptide, determined from proton two-dimensional nuclear magnetic resonance data, Eur. J. Biochem. 256 (1998) 404-410.

[13] N. Mandard, P. Bulet, A. Caille, S. Daffre, F. Vovelle, The solution structure of gomesin, an antimicrobial cysteine-rich peptide from the spider, Eur. J. Biochem. 269 (2002) 1190-1198.

[14] W. Gong, J. Wang, Z. Chen, B. Xia, G. Lu, Solution structure of LCl, a novel antimicrobial peptide from *Bacillus subtilis*, Biochemistry 50 (2011) 3621-3627.

[15] Y. Huang, J. Huang, Y. Chen, Alpha-helical cationic antimicrobial peptides: relationships of structure and function, Protein Cell 1 (2010) 143-152.

[16] M.J. Chrispeels, N.V. Raikhel, Lectins, lectin genes, and their role in plant defense, Plant Cell 3 (1991) 1-9.

[17] N.V. Raikhel, H.I. Lee, W.F. Broekaert, Structure and functions of chitin-binding proteins, Ann. Rev. Plant Physiol. Plant Mol. Biol. 44 (1993) 591-615.

[18] T. Nakamura, H. Furunaka, T. Miyata, F. Tokunaga, T. Muta, S. Iwanaga, M. Niwa, T. Takao, Y. Shimonishi, Tachyplesin, a class of antimicrobial peptide from the hemocytes of the horseshoe crab (*Tachypleus tridentatus*). Isolation and chemical structure, J. Biol.

Chem. 263 (1988) 16709-16713.

[19] K. Kawano, T. Yoneya, T. Miyata, K. Yoshikawa, F. Tokunaga, Y. Terada S. Iwanaga, Antimicrobial peptide, tachyplesin I, isolated from hemocytes of the horseshoe crab (*Tachypleus tridentatus*). NMR determination of the beta-sheet structure, J. Biol. Chem. 265 (1990) 15365-15367.

[20] A.G. Rao, Conformation and antimicrobial activity of linear derivatives of tachyplesin lacking disulfide bonds, Arch. Biochem. Biophys. 361 (1999) 127-134.

[21] S. Kawabata, Horseshoe crab antimicrobial proteins with chitin-binding activity, Tanpakushitsu Kakusan Koso 46 (2001) 388-394.

[22] J.P. Powers, A. Rozek, R.E. Hancock, Structure-activity relationships for the beta-hairpin cationic antimicrobial peptide polyphemusin I, Biochim. Biophys. Acta 1698 (2004) 239-250.

[23] F. Delaglio, S. Grzesiek, G.W. Vuister, G. Zhu, J. Pfeifer, A. Bax, NMRPipe: a multidimensional spectral processing system based on UNIX pipes, J. Biomol. NMR. 6 (1995) 277-293.

[24] T.D. Goddard, D.G. Kneller, SPARKY 3, University of California, San Francisco, 2006

[25] L. Braunschweiler, R.R. Ernst, Coherence transfer by isotropic mixing: Application to proton correlation spectroscopy, J. Magn. Reson. 53 (1983) 521–528.

[26] S. Kawabata, R. Nagayama, M. Hirata, T. Shigenaga, K.L. Agarwala, T. Saito, J. Cho, H. Nakajima, T. Takagi, S. Iwanaga, Tachycitin, a small granular component in horseshoe crab hemocytes, is an antimicrobial protein with chitin-binding activity, J. Biochem. 120 (1996) 1253-1260.

[27] A. Laederach, A.H. Andreotti, D.B. Fulton, Solution and micelle-bound structures of tachyplesin I and its active aromatic linear derivatives, Biochemistry 41 (2002) 12359-12368.

[28] D. Marion, M. Zasloff, A. Bax, A two-dimensional NMR study of the antimicrobial

peptide magainin 2, FEBS Lett. 227 (1988) 21-26.

[29] H.C. Chen, J.H. Brown, J.L. Morell, C.M. Huang, Synthetic magainin analogues with improved antimicrobial activity, FEBS Lett. 236 (1988) 462-466.

[30] D.J. Schibli, P.M. Hwang, H.J. Vogel, Structure of the antimicrobial peptide tritrpticin bound to micelles: a distinct membrane-bound peptide fold, Biochemistry 38 (1999) 16749-16755.

[31] A. Szyk, Z. Wu, K. Tucker, D. Yang, W. Lu, J. Lubkowski, Crystal structures of human alpha-defensins HNP4, HD5, and HD6, Protein Sci. 15 (2006) 2749-2760.

[32] T. Suetake, T. Aizawa, N. Koganesawa, T. Osaki, Y. Kobashigawa, M. Demura, S. Kawabata, K. Kawano, S. Tsuda, K. Nitta, Production and characterization of recombinant tachycitin, the Cys-rich chitin-binding protein, Protein Eng. 15 (2002) 763-769.

[33] T. Osaki, M. Omotezako, R. Nagayama, M. Hirata, S. Iwanaga, J. Kasahara, J. Hattori, I. Ito, H. Sugiyama, S. Kawabata, Horseshoe crab hemocyte-derived antimicrobial polypeptides, tachystatins, with sequence similarity to spider neurotoxins, J. Biol. Chem. 274 (1999) 26172-26178.

[34] J. Van Parijs, W.F. Broekaert, I.J. Goldstein, W.J. Peumans, Hevein: an antifungal protein from rubber-tree (*Hevea brasiliensis*) latex, Planta 183 (1991) 258-264.

[35] J.L Asensio, F.J. Cañada, M. Bruix, A. Rodríguez-Romero, J. Jiménez-Barbero, The interaction of hevein with N-acetylglucosamine-containing oligosaccharides. Solution structure of hevein complexed to chitobiose, Eur. J. Biochem. 230 (1995) 621-633.

[36] J.L Asensio, F.J. Cañada, M. Bruix, C. González, N. Khiar, A. Rodríguez-Romero, J. Jiménez-Barbero, NMR investigations of protein-carbohydrate interactions: refined three-dimensional structure of the complex between hevein and methyl beta-chitobioside, Glycobiology, 8 (1998) 569-577.

[37] J.L Asensio, F.J. Cañada, H.C. Siebert, J. Laynez, A. Poveda, P.M. Nieto, U.M.

Soedjanaamadja, H.J. Gabius, J. Jiménez-Barbero, Structural basis for chitin recognition by defense proteins: GlcNAc residues are bound in a multivalent fashion by extended binding sites in hevein domains, Chem. Biol. 7 (2000) 529-543.

[38] N. Aboitiz, M. Vila-Perelló, P. Groves, J.L Asensio, D. Andreu, F.J. Cañada, J. Jiménez-Barbero, NMR and modeling studies of protein-carbohydrate interactions: synthesis, three-dimensional structure, and recognition properties of a minimum hevein domain with binding affinity for chitooligosaccharides, Chembiochem 5 (2004) 1245-1255.

[39] T. Suetake, S. Tsuda, S. Kawabata, K. Miura, S. Iwanaga, K. Hikichi, K. Nitta, K. Kawano, Chitin-binding proteins in invertebrates and plants comprise a common chitin-binding structural motif, J. Biol. Chem. 275 (2000) 17929-17932.

[40] N. Fujitani, S. Kawabata, T. Osaki, Y. Kumaki, M. Demura, K. Nitta, K. Kawano, Structure of the antimicrobial peptide tachystatin A, J. Biol. Chem. 277 (2002) 23651-23657.

[41] N. Fujitani, T. Kouno, T. Nakahara, K. Takaya, T. Osaki, S. Kawabata, M. Mizuguchi, T. Aizawa, M. Demura, S. Nishimura, K. Kawano, The solution structure of horseshoe crab antimicrobial peptide tachystatin B with an inhibitory cysteine-knot motif, J. Pept. Sci. 13 (2007) 269-279.

[42] W.L. DeLano, The PyMOL Molecular Graphics System, Version 1.6.0.0 Schrödinger, LLC, 2013.

Table 1. Primary sequence of TP I mutants.

TP(F4A)	KWCARVCYRGICYRRCR-NH2
TP(R9A)	KWCFRVCYAGICYRRCR-NH2
TP(Y13A)	KWCFRVCYRGICARRCR-NH2
TP(R17A)	KWCFRVCYRGICYRRCA-NH2
TP(F4A Y13A)	KWCARVCYRGICARRCR-NH2
TP(R9A R17A)	KWCFRVCYAGICYRRCA-NH2
TP(F4A R9A Y13A R17A)	KWCARVCYAGICARRCA-NH2
TP(C3A C7A C12A C16A)	KWAFRVAYRGIAYRRAR-NH2

(a)

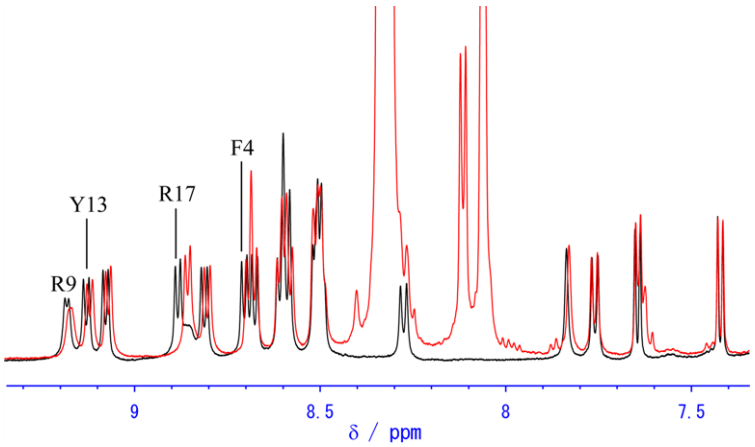

(b)

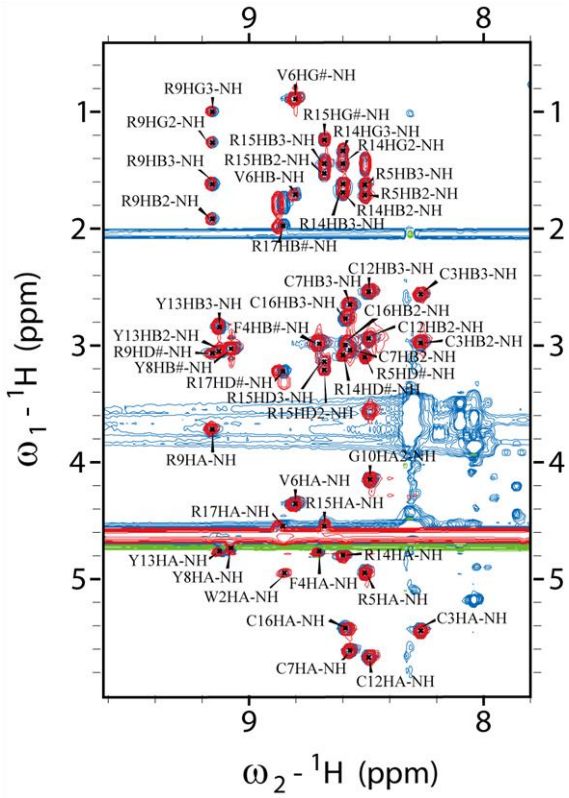

Figure 1. (a) Superimposition of the 1D ^{1}H NMR spectra of TP I in the presence (red) and absence (black) of chitohexaose. (b) Superimposition of the TOCSY spectra of TP I with (red) or without (blue) chitohexaose.

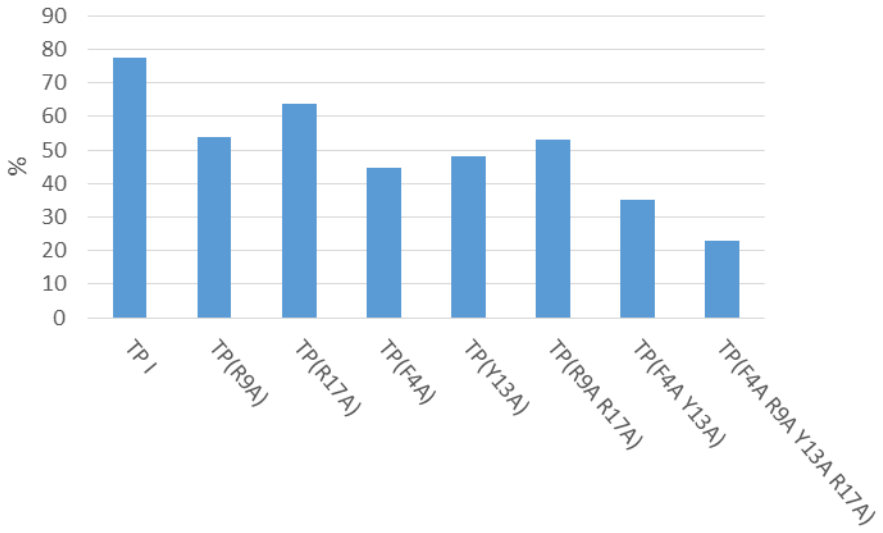

Figure 2. Content rate of peptides in eluted solution. The sum total of peptide in the flow-through solution and eluted solution was defined as 100%.

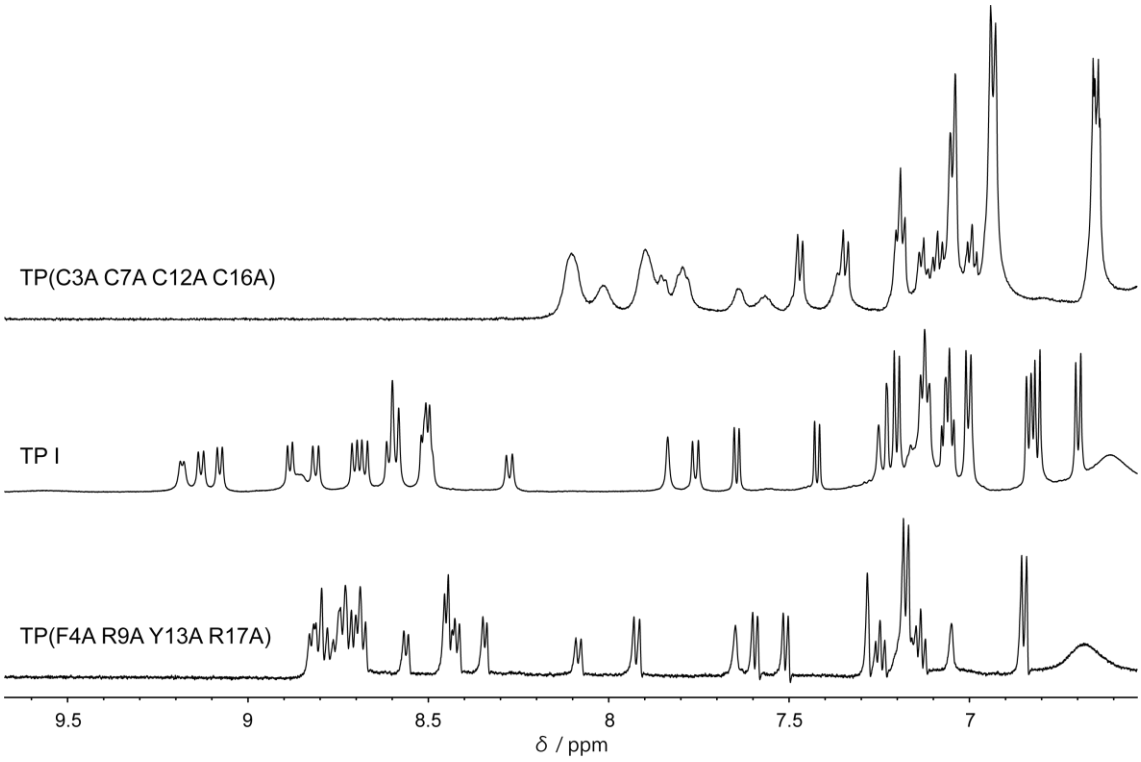

Figure 3. Low-filed resonance of the 1D ^{1}H NMR spectra of TP(C3A C7A C12A C16A) (top), TP I (middle) and TP(F4A R9A Y13A R17A) (bottom).

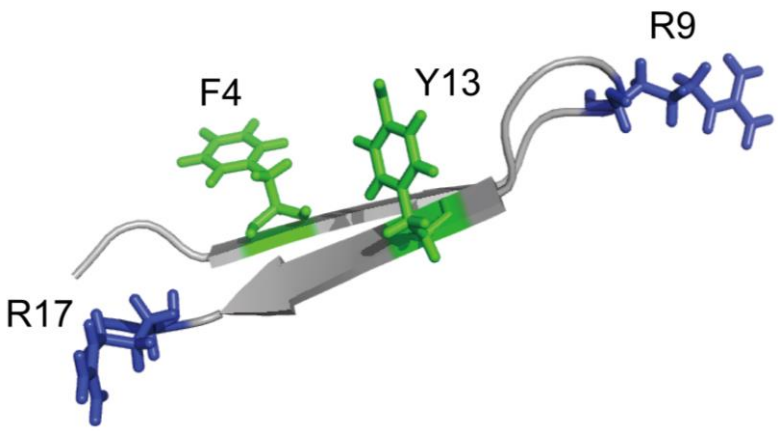

Figure 4. Cartoon representation of the TP I structure. Key residues that are expected to be involved in binding to chitin are shown as sticks. The green color represents aromatic residues and blue color represents cationic residues. The structure was visualized using PyMOL software [42].

Concluding Remarks

In this thesis I showed the details of the interaction between AMPs and substances derived from pathogens, LPS and chitin.

In Part I of this thesis, I investigated the structure of TP I, which is isolated from horseshoe crab in the presence of LPS, a major substance of Gram-negative bacteria. In addition, I proposed a structural model of the complex between them.

First, I measured the CD spectra and NMR spectra of TP I in the presence and absence of LPS and revealed that TP I extends its β-sheet structure and stabilizes this structure by binding to LPS. I also revealed that Trp2 of TP I is important for the binding to LPS. Fluorescence studies indicated that Trp2 is incorporated into the hydrophobic area of LPS, and 1D ^{1}H NMR suggested that Trp2 is involved in the binding to LPS. Further, NMR studies showed the importance of the phosphate groups of LPS in binding to TP I. The complex structure obtained by docking calculation between TP I and LPS showed that TP I lies across the two GlcNs of LPS. In the complex, the cationic Lys1, Arg15 and Arg17 residues interact with the phosphate groups or saccharides of LPS, whereas the aromatic residues Trp2 and Phe4 interact with the acyl chains of LPS.

By binding to LPS, TP I seems to twist its antiparallel β-sheet structure. I considered that this twisting β-sheet structure may be important for TP I to recognize LPS. In the case of AMPs categorized into the α-helical type, they drastically change their structure in the membrane. Although the structures of most β-sheet type AMPs are stabilized by disulfide bonds and cannot drastically change, slight changes in structure may endow β-sheet AMPs with LPS-binding ability.

In Part II of this thesis, I investigated the structural factors or key residues that are important for the binding of TP I to chitin, a major component of the fungal cell wall. From the 1D ^{1}H NMR spectra of TP I with or without hexa-N-acetyl-chitohexaose, it was clearly

confirmed that the HN chemical shifts of F4, R9, Y13, and R17 are changed by the addition of hexa-N-acetyl-chitohexaose. This indicated that the F4, R9, Y13 and R17 residues of TP I may have the ability to interact with hexa-N-acetyl-chitohexaose. Then, a chitin-binding assay was performed using TP I and its mutants to investigate the effect of four residues on the chitin-binding ability. The results of this assay indicated that the aromatic F4 and Y13 residues are more important for the binding to chitin than the cationic residues R9 and R17. In the structure of TP I, the side chains of these four residues are in the same plane of the β-sheet. One surface formed by these four residues may recognize chitin. I consider that the local region formed by F4 and Y13 plays the main role in the binding to chitin, while R9 and R17 interact with chitin only secondarily.

Next, I measured the 1D ^{1}H NMR spectrum of TP(F4A R9A Y13A R17A) to predict its conformation and confirmed that the peptide adopts a well-defined structure. In other words, TP(F4A R9A Y13A R17A) hardly bound to chitin although it adopted a secondary structure.

To my knowledge, TP I is the shortest antimicrobial peptide that exhibits chitin-binding activity. My findings in this study should assist in clarification of the mechanism of chitin-recognition of AMPs and in elucidation of the relationship between antifungal activity and chitin-binding activity.

Acknowledgements

This work was supported by JSPS KAKENHI Grant Number 25–2798.

I gratefully acknowledge the invaluable suggestions and support of Professor Keiiichi Kawano and Associate Professor Tomoyasu Aizawa. I would also like to express my gratitude to Professor Makoto Demura, Lecturer Takashi Kikukawa, Assistant Professor Masakatsu Kamiya and Dr. Yasuhiro Kumaki for their fruitful suggestions and support.

I also deeply appreciate the efforts of Professor Min Yao in reviewing this paper.

I am deeply indebted to my family for their many avenues of support. They have always sustained me and encouraged me to pursue my passions. I also express my deepest gratitude to my friends. They have always cared about and promoted my growth in life and academia. Finally, I am grateful to the many colleagues and associates who have fostered my 9-year journey at Hokkaido University.